

DOE/ET-53088-307

IFSR #307

**WKB Theory of Wave Tunneling
for Hermitian Vector Systems
of Integral Equations**

*H. J. Kull, R. J. Kashuba,
and H. L. Berk*

Institute for Fusion Studies
The University of Texas at Austin
Austin, Texas 78712

January 1988

Errata

IFSR 307

p. 17: 9 lines from the bottom "...and less..." should read
"...and greater...".

p. 19: Equation (38) should read,

$$\begin{aligned}
 A^{-}(\rightarrow \bullet) + A^{+}(\bullet \leftarrow) &\xrightarrow{S_1} A^{-}(\downarrow \bullet + \curvearrowright \bullet) + A^{+}(\bullet \uparrow) \\
 &\xrightarrow{S_2} A^{+}(\bullet \uparrow + \frac{1}{2} \bullet \downarrow) + A^{-}(\curvearrowleft \bullet + \downarrow \bullet + \frac{1}{2} \bullet \curvearrowright) \\
 &= A^{+}(\bullet \uparrow + \frac{1}{2} \bullet \downarrow) + A^{-}(\curvearrowleft \bullet + \frac{1}{2} \downarrow \bullet)
 \end{aligned}$$

p. 20: Equation (42), first equation "... D_b ..." should be
"... D_a ...".

WKB Theory of Wave Tunneling for Hermitian Vector Systems of Integral Equations

H.J. Kull^{a)}, R.J. Kashuba^{b)}, H.L. Berk

Institute for Fusion Studies
The University of Texas at Austin
Austin, Texas 78712

Abstract

A general theory of wave tunneling in one dimension for Hermitian vector systems of integral equations is presented. It describes mode conversion in terms of the general dielectric tensor of the medium, and without regard to specific models gives a proper account to the forward and backward nature of the waves. Energy conservation in the WKB approximation can be obtained for general linear systems by a consistent treatment of the vector polarization and by the use of modified Furry rules, which are similar to those used by Heading for second order differential equations. Operational graphical rules are developed to construct global wave solutions and to determine the direction of energy flow for spatially disconnected roots. In principle these rules could be applied to systems with arbitrary mode complexity. Coupling coefficients for wave tunneling problems with up to four interacting modes are calculated explicitly.

^{a)}Institut für Angewandte Physik, Technische Hochschule, 6100 Darmstadt (FRG)

^{b)} McDonnell Douglas Corporation, Astronautics-Eastern Div., P. O. Box 516,
St. Louis, Missouri 63166

1 Introduction

Wave tunneling is a well-known phenomenon, which allows waves to penetrate into regions which would not be accessible along their ray trajectories. This effect has been particularly well studied for second order equations in the quantum mechanical context.¹ More generally tunneling can occur for higher order equations, a problem, that is of particular importance for mode conversion in magnetized plasmas.² In this paper we wish to examine the general tunneling problem for Hermitian vector systems of integral equations in the WKB approximation. As a special case this formulation includes Hermitian differential operators of arbitrary high order. The primary motivation for this study comes from the linear Vlasov-Maxwell theory, which leads to Hermitian operators when particle resonances are not present or neglected, e.g. for wave propagation perpendicular to the magnetic field.³⁻⁴ As a consequence of Hermiticity the total wave energy flow is exactly conserved.⁵⁻⁶ It is therefore a basic goal of the present treatment to obtain consistency with wave energy conservation.

In the geometrical optics approximation waves propagate along rays, which are determined by spatially varying wave numbers $k(x)$ along the inhomogeneity direction x . Tunneling occurs across narrow spatial regions, which separate two or more branches for the wave numbers. Across these regions the usual geometrical optics approximation fails and couplings occur between the individual waves. The mode conversion tunneling problem consists in the determination of the various coupling coefficients that arise between the in- and outgoing waves at the boundaries of the medium.

Previous work has been mostly based on specific model equations for tunneling regions. Mode conversion in thermal plasmas has been studied particularly well by certain fourth-order equations with linearly varying coefficients.^{2,7-9} Attempts to formulate unified descriptions of pairwise coupling have led to further model representations by second-order differential equations¹⁰⁻¹¹ and systems of coupled first-order equations.¹²⁻¹⁴ In the present treatment we consider general linear systems and carefully discuss the aspect of wave energy conservation. For this purpose we apply

and extend WKB techniques developed for higher order equations.¹⁵⁻¹⁷ This approach is advantageous, since the tunneling problem can be discussed in terms of the general dielectric tensor of the homogeneous medium, which is regarded as a known quantity. Furthermore it allows in principle to deal with arbitrary tunneling structures and mode complexity in slowly varying media.

The WKB formulation provides a general way of determining the energy flow direction of the outgoing waves relative to the incident flow. It is found, that in general the vector representation is important to obtain the proper orientation of the energy flow, and we show, how the vector polarization determines the forward and backward nature of the waves.

We also develop a graphical operational procedure based on modified Furry rules, that enables one to describe the coupling between the waves in the mode conversion tunneling problem. The wave amplitudes are represented by isomorphic diagrams for the complex wave numbers and a multiplication is defined, that allows to propagate waves by observing some basic operational rules.

Energy conservation in the WKB theory is achieved by a modified Furry rule for the wave representation inside a tunneling region. This rule has been discussed by Heading for second-order differential equations.¹⁸ Previously phase integral methods have been applied for determining generalized Furry rules for higher order equations.¹⁵⁻¹⁶ Following these methods the modified Furry rule can be explained by a bifurcation of the steepest descent path on Stokes' lines. In addition, this rule is shown to conserve wave energy for general tunneling structures. The general formulation of the mode coupling rules by graphical methods and its resulting energy conservation is the principal result of this work.

The paper is organized as follows. In Sec.2 the present WKB techniques are introduced. The wave diagrams and Furry rules are explained and subsequently used to demonstrate consistency with wave energy conservation. In Sec.3 we use this formalism to analyse conventional tunneling through a potential barrier and make comparison with an exact solution. In Sec.4 we treat mode conversion between waves, which tunnel with a non-zero real part of the wave numbers. Finally, in Sec.5

representative cases of the four wave tunneling problem are considered, that describes mode-conversion near ion-cyclotron frequencies.^{5,9,19}

2 WKB Method

In this section we define the general rules to construct global solutions to the tunneling problem. These rules generalize usual Furry rules and are expressed by wave diagrams, that allow one to determine graphically the change of wave amplitudes. By observing these rules consistency with wave energy conservation is obtained in the WKB theory.

A Local dispersion relation

We consider the propagation of waves with a frequency ω in a Vlasov-Maxwell system with spatial variations along the x direction. The electric field $\mathbf{E}(x)$ is governed by a vector system of integral equations of the general form,

$$\int dx' \mathbf{K}(x, x') \cdot \mathbf{E}(x') = 0. \quad (1)$$

Here and in the following the dependence on the constant frequency and a constant wave vector perpendicular to the x direction is suppressed in the notation. We will neglect dissipation by assuming that the matrix elements of the kernel have the Hermiticity property that $K_{ij}(x, x') = K_{ji}^*(x', x)$.

For systems with weak inhomogeneities the WKB method determines asymptotic solutions of Eq.(1). The dielectric tensor of the medium can be introduced as the Fourier transform of the integral kernel with respect to the difference of its arguments,¹⁵⁻¹⁷

$$\mathbf{D}(x,k) = \int dq \mathbf{K}(x + \frac{q}{2}, x - \frac{q}{2}) e^{-ikq} . \quad (2)$$

The wave solutions are characterized by local wave numbers $k = k(x)$, which are roots of the local dispersion relation,

$$\Lambda(x,k) = \det |D_{ij}(x,k)| = 0 . \quad (3)$$

This is generally a transcendental equation and we assume, that $\Lambda(z,k)$ is an entire function of complex variables z and k . According to complex analysis it can then be represented by its zeros in the product form,²⁰

$$\Lambda(z,k) = e^{g(k)} k^m \prod_n (1 - \frac{k}{k_n}) e^{p_n(k)} . \quad (4)$$

Here z is considered fixed, $g(k)$ represents an entire function, $p_n(k)$ are convergence producing polynomials, m is the multiplicity of the zero $k = 0$ and n labels all zeros $k_n \neq 0$. The number of zeros can be zero, finite or infinite. In the following we assume, that all zeros are distinct in the asymptotic regions $|x| \rightarrow \infty$ and coalesce only pairwise elsewhere. From Eq.(4) the condition for pairwise coalescence is found to be,

$$\Lambda(z,k) = \Lambda_{,k}(z,k) = 0 ; \quad \Lambda_{,k,k}(z,k) \neq 0 , \quad (5)$$

where $\Lambda_{,k}$ denotes the partial derivative with respect to k .

If z varies in the complex plane a branch $k = k_n(z)$ of the dispersion relation (3) becomes in general a multi-valued function of z . To determine the analytic continuation of a given branch it is convenient to consider a parameter representation $z(\tau)$, $k(\tau)$ of the zeros with a complex variable τ . In analogy with the real Hamiltonian ray equations the functions $z(\tau)$ and $k(\tau)$ are determined by the system,

$$\frac{dz}{d\tau} = \Lambda_{,k} \quad , \quad \frac{dk}{d\tau} = -\Lambda_{,z} \quad . \quad (6)$$

Since $\Lambda(z,k)$ is assumed analytic, there exists a unique analytic solution to initial conditions $z(\tau_0) = z_0$, $k(\tau_0) = k_0$ at $\tau = \tau_0$. We now choose $\Lambda(z_0, k_0) = 0$ and a path in the τ -plane such, that $z(\tau)$ maps on a given path in the z -plane. The branch $k = k(z)$ then is uniquely defined by the corresponding values of $k(\tau)$. The continuation of a given branch can therefore be reduced to the solution of an initial value problem. The WKB solutions in the complex plane depend on these trajectories and their behavior around branch points.

A branch point z_B , k_B of $k = k(z)$ occurs when $\Lambda_{,k} = 0$. Expanding about z_B, k_B the solution of Eq.(6) is obtained locally in the form,

$$\delta k = \delta s \quad , \quad \delta z = -\frac{1}{2} \frac{\Lambda_{,k,k}}{\Lambda_{,z}} \delta s^2 \quad , \quad (7)$$

with $\delta k = k - k_B$, $\delta z = z - z_B$, and $\delta s = -\Lambda_{,z}(\tau - \tau_B)$. If we propagate δz around the branch point a phase change $\delta\psi$ of δz is accompanied by a phase change $\delta\psi/2$ of δk . This rule is useful to gain a qualitative picture of the behavior of wave trajectories. Analogously a branch point of the inverse function $z = z(k)$ occurs when $\Lambda_{,z} = 0$ and here the phase change of δk is found to be $2\delta\psi$.

B Local asymptotic solutions

The local asymptotic solutions of Eq.(1) assume the well-known form,¹⁵

$$\mathbf{E}(z) = \mathbf{a}(z) e^{iS(z)} \quad . \quad (8)$$

The exponent $S(z)$ represents the rapidly varying function,

$$S(z) = S(z_0) + \int_{z_0}^z dz' k(z') \quad . \quad (9)$$

For Hermitian operators the solution for the components of the vector amplitude can be represented in the form,

$$a_i(p) = \frac{C_{if}}{C_{ff}} a_f(p) \quad , \quad a_f(p) = \left(\frac{D_{,k}(p_0)}{D_{,k}(p)} \right)^{1/2} a_f(p_0) \quad , \quad (10)$$

with the definitions,

$$\mathbf{D} \cdot \mathbf{C} = \Lambda \mathbf{I} \quad , \quad \mathbf{D} = \Lambda / C_{ff} \quad , \quad p \equiv (z, k(z)) \quad . \quad (11)$$

Here \mathbf{I} denotes the unit tensor, \mathbf{C} the transposed matrix of the cofactors of \mathbf{D} and for simplicity the dependence on z and $k(z)$ is expressed by a single variable p . For $\Lambda = 0$ one of the columns of \mathbf{C} with an arbitrary but fixed index f has been used to express the components of the solution vector in Eq.(10). It is then sufficient to describe the variation of the single scalar quantity a_f . We remark, that the main difference between a scalar equation and a vector system lies in the appearance of the cofactor C_{ff} in the expression for D . For scalar equations one can set $C_{ff} = 1$ and therefore $D = \Lambda$ in Eq.(10).

C Diagram representation

We now develop a graphical procedure to construct WKB solutions of the mode coupling problem. For this purpose a diagram representation of WKB waves is introduced and basic operational rules are defined, that allow to determine mode coupling coefficients graphically.

We propagate the vector component $E_f(z)$ as defined by Eqs.(8)-(11) along a complex path from p_1 to p_2 thereby avoiding branch-points. The ratio $E_f(p_2)/E_f(p_1)$ then is written in the form,


$$\langle k|1,2\rangle = a(k|1,2) e^{i[-\frac{1}{2} \delta(k|1,2) + S(k|1,2)]} \quad (12)$$

with

$$a(k|1,2) = \left| \left(\frac{D_{,k}(p_1)}{D_{,k}(p_2)} \right)^{1/2} \right|,$$

$$\delta(k|1,2) = \arg \left(D_{\mathbf{k}}(p) \right) \Big|_{p_1}^{p_2}, \quad S(k|1,2) = S(p) \Big|_{p_1}^{p_2}.$$

This expression is uniquely determined by the path of $k = k(z)$ in the complex k -plane and by the end-points $p_{1,2}$. We therefore represent the WKB wave $\langle k|_{1,2}\rangle$ by an isomorphic diagram,

$$\langle k | 1, 2 \rangle \equiv$$


$$(13)$$

It indicates schematically the path in the k -plane, the direction of propagation (arrow) and the end-points (indices). Horizontal and vertical dashed lines represent the real and imaginary k axis, respectively. We now introduce a product of diagrams by defining,

$$\langle k|1,2\rangle\langle k'|3,4\rangle \equiv \begin{array}{c} \text{---} \curvearrowright \text{---} \\ | \quad 2 \end{array} \circ \begin{array}{c} \text{---} \curvearrowright \text{---} \\ | \quad 3 \end{array} \quad (14)$$

Without ambiguity we can often suppress the coordinate lines, the indices and the multiplication symbol \circ for simplicity of notation.

We now discuss some basic graphical operations for wave diagrams. If the wave amplitude (12) is propagated from point 1 to point 3 across an intermediate point 2, there holds the multiplication rule, $\langle k|1,2\rangle \langle k|2,3\rangle = \langle k|1,3\rangle$. This property is expressed graphically in the form,

$$\begin{array}{c} \text{2} \quad \text{2} \\ \curvearrowright \quad \curvearrowright \\ 1 \quad \quad 3 \end{array} \circ = \begin{array}{c} \curvearrowright \\ 1 \quad \quad 3 \end{array} \quad (15)$$

The inverse of a diagram is obtained by reversing the direction of propagation,

$$\begin{array}{c} \curvearrowright \\ 1 \quad \quad 2 \end{array} \circ \begin{array}{c} \curvearrowleft \\ 1 \quad \quad 2 \end{array} = | \quad (16)$$

or

$$\left(\begin{array}{c} \curvearrowright \\ 1 \quad \quad 2 \end{array} \right)^{-1} = \begin{array}{c} \curvearrowleft \\ 1 \quad \quad 2 \end{array} \quad (17)$$

Branch-points where $\Lambda_k = 0$ are symbolized by a dot. Propagating δk around a branch-point we obtain from Eq.(12) for a complete circle that $\delta(k|1,2) = \pm 2\pi$. The plus sign corresponds to counterclockwise and the minus sign to clockwise rotation. A branch-point, where $\Lambda_z = 0$ is symbolized by a cross, and here the amplitude (12) is analytic. The phase rules for encircling branch-points are expressed by the diagrams,

$$\begin{array}{c} \circlearrowleft \\ \bullet \end{array} = e^{-i\pi}, \quad \begin{array}{c} \circlearrowleft \\ \times \end{array} = 1 \quad (18)$$

To define further graphical rules we will now assume the common relations $D(z, -k) = D(z, k)$ and $D^*(z, k) = D(z^*, k^*)$ for $D(z, k)$ as defined in Eq.(11). The first relation is satisfied, if the determinant Λ and the diagonal elements of the dielectric tensor are even functions of k . We are therefore dealing with media, where waves with opposite signs of k propagate with opposite group velocities $v_{gr} \sim \Lambda_k$. The second relation is a consequence of the reflection principle for analytic functions²⁰, if $D(z, k)$ is assumed real for real arguments.

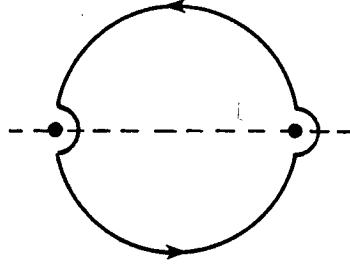
Let us now consider a product of two diagrams, which are symmetric with respect to the origin,

$$(19)$$

The two diagrams represent waves with wave numbers k and $-k$ and with end-points $1 \equiv (k_1, z_1)$, $2 \equiv (k_2, z_2)$, $-1 \equiv (-k_1, z_1)$, $-2 \equiv (-k_2, z_2)$. According to Eq.(12) they are related by $a(-k|-1, -2) = a(k|1, 2)$, $\delta(-k|-1, -2) = \delta(k|1, 2)$, $S(-k|-1, -2) = -S(k|1, 2)$. The product diagram (19) therefore has the value,

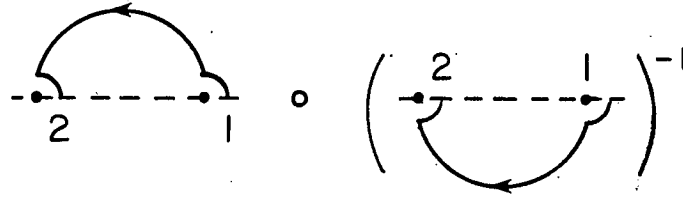
$$\langle k|1,2\rangle \langle -k|-1,-2\rangle = \frac{D_{,k}(1)}{D_{,k}(2)} \quad (20)$$

Another diagram, that occurs frequently, is given by a closed loop around two branch-points on the real axis,



(21)

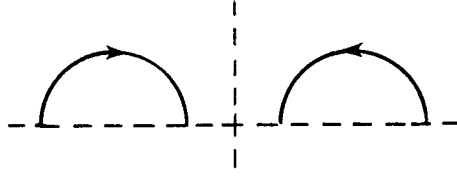
Alternatively, using Eq.(17), this diagram can be represented by the product,



One has then to take the ratio between two diagrams, which are symmetric to the real axis. Reflection at the real axis is obtained by substituting $k \rightarrow k^*$ and $z \rightarrow z^*$. From Eq.(12) one finds the corresponding relations, $a(k^*|1,2) = a(k|1,2)$, $\delta(k^*|1,2) = -\delta(k|1,2)$, $S(k^*|1,2) = -S^*(k|1,2)$. The loop diagram then can be evaluated as,

$$\frac{\langle k | 1,2 \rangle}{\langle k^* | 1,2 \rangle} = \sigma e^{i \oint k dz}, \quad \sigma = e^{-i \delta(k|1,2)} = \text{sgn} \left(\frac{D_{,k}(1)}{D_{,k}(2)} \right), \quad (22)$$

where $\text{sgn}(x) = \pm 1$ corresponding to the sign of x and the integration path is taken along the loop. We finally discuss the product of two diagrams, which are symmetric with respect to the imaginary axis,



Reflection at the imaginary axis $k \rightarrow -k^*$ combines the symmetries $k \rightarrow -k$ and $k \rightarrow k^*$, yielding $a(-k^*|-1,-2) = a(k|1,2)$, $\delta(-k^*|-1,-2) = -\delta(k|1,2)$, $S(-k^*|-1,-2) = S^*(k|1,2)$. Accordingly, the waves $\langle k|1,2 \rangle$ and $\langle -k^*|-1,-2 \rangle$ represent complex conjugate solutions. Their product gives the squared magnitude of each diagram and can be expressed by a diagram of the form (19) times a loop diagram (21),

This representation is particularly useful to evaluate energy expressions of wave solutions. We now have summarized the basic graphical identities, that will be used in the subsequent sections.

D Construction of Tunneling Solutions

In this section phase integral methods are used to obtain an asymptotic representation of the solution inside wave tunneling regions. The result is expressed as a modified Furry rule, that allows to construct global tunneling solutions. We shall first present the rules and then justify them using a phase integral steepest descent method.

Asymptotically as $|x| \rightarrow \infty$ we assume homogeneous regions, where the solution is represented by propagating and evanescent plane waves. The aim is to relate the wave amplitudes at $x \rightarrow +\infty$ to those at $x \rightarrow -\infty$ if these regions are separated by an inhomogeneous tunneling structure. The tunnel region is assumed to consist of two or more separated branch-points x_B , where the mode coupling condition $\Lambda(x_B, k_B) = \Lambda, k(x_B, k_B) = 0$ is satisfied. At each point x_B, k_B two roots $k_{1,2}$ coalesce and the corresponding WKB solutions (8) fail. Passing around these points in the complex z -plane a change in the asymptotic representation can take place across Stokes' lines, which are defined by the condition,¹⁵⁻¹⁸

$$\text{Im} \left(i \int_{x_B}^z (k_1 - k_2) dz' \right) = 0 \quad (24)$$

and form locally a star with three rays intersecting at x_B under an angle $2\pi/3$ (Fig.1). On a Stokes' line the ratio between the two solutions acquires a purely real exponential factor. The exponentially large solution is called dominant and the exponentially small solution subdominant. In the tunneling problems we consider, one of the Stokes' lines is directed along the real axis. In general this requires, according to Eqs.(7) and (24), that x_B and k_B^2 are taken real. As shown in Fig.1 we indicate the dominant wave on each Stokes' line by the corresponding sign of $\text{Im}(\delta k)$.

The change of the asymptotic representation across a Stokes' line is expressed by the following Furry rule: If a dominant wave is propagated across a Stokes' line, one has to add a subdominant solution, which is the analytic continuation of the dominant wave around the branch-point in the opposite sense of propagation. This rule can be readily represented by diagrams. In Fig.1 we propagate the dominant wave with $\text{Im}(\delta k) < 0$ across S_1 . According to Eq.(7) δk rotates in the same sense as δz but only by half the angle. This gives rise to the graphical connection formula,

(25)

The l.h.s. represents the wave before and the r.h.s. after the crossing of the Stokes' line, which occurs in the k -plane at an angle $\pi/6$ with the real axis. The subdominant wave is obtained by backward propagation at the Stokes' line.

To deal with wave propagation along the Stokes' line on the real axis, we now formulate a second modified Furry rule, which has been discussed by Heading for second-order equations.¹⁸ If a dominant wave is propagated on or off a Stokes' line, without actually crossing it, only one half of the subdominant wave as determined by the usual Furry rule has to be added. In terms of diagrams this rule assumes the form,

(26)

The Stokes' phenomenon described so far can be examined for higher order equations by phase integral methods.¹⁵⁻¹⁶ The starting point here is a contour integral representation of the solution,

$$\mathbf{E}(z) = \frac{1}{\sqrt{2\pi i}} \int_C dk \, \hat{\mathbf{E}}(k) e^{ikz}, \quad (27)$$

where the contour C connects two remote regions in the k -plane where the integrand vanishes. Usually there exist as many independent contours as independent solutions.

For the dual vector field $\hat{\mathbf{E}}(k)$ asymptotic solutions have been derived, which assume the form,¹⁵

$$\hat{E}_i(k) = \left(\frac{C_{if}}{C_{ff}} \frac{1}{\sqrt{D_{,z}}} \right) \Big|_{z=z(k)} e^{-i\hat{S}(k)} , \quad (28)$$

$$\hat{S}(k) = \hat{S}(k_0) + \int_{k_0}^k z(k') dk' .$$

The dual representation (28) fails near the branch-points of $z = z(k)$, however, it is accurate near those of $k = k(z)$. One can therefore use this representation to obtain asymptotic expansions near the mode-coupling points in x -space. According to the method of steepest descent the contour C is deformed into a steepest descent path across saddle points. The saddle points follow from the condition,

$$\frac{d}{dk} \left(kz - \int_{k_0}^k z(k') dk' \right) = z - z(k) = 0 , \quad (29)$$

and are coincident with the roots of the local dispersion relation at the point z . Performing the integration across the saddle at $k=k(z)$ along the direction $e^{i\varphi}$ of the steepest descent path, the contribution to the contour integral is found to be,

$$E_i(z) = \left(\frac{C_{if}}{C_{ff}} \frac{1}{\sqrt{D_{,k}}} \right) \Big|_{k=k(z)} e^{iS(z)} , \quad (30)$$

with the branch of the square root defined by,

$$\left(\frac{\Lambda_{,k}}{\Lambda_{,z}} \right)^{1/2} e^{i(\varphi-\pi/4)} > 0 .$$

In this way there follows for each saddle crossed by the contour C the corresponding WKB solution in x -space.

In the Appendix we shall show how the Furry rule given by Eq. (26) is derived.

E Energy conservation

We now address some issues of wave energy conservation in the wave tunneling context. First generalized mode coupling coefficients are defined, that express global energy conservation, then the direction of energy flow for spatially disconnected roots is specified, and finally consistency of the modified Furry rules with wave energy conservation is demonstrated.

At the boundaries $|x| \rightarrow \infty$ the solution is taken as a superposition of WKB waves and in accordance with our symmetry assumptions in the local dispersion relation the wave numbers occur in pairs of $k, -k$ and k, k^* . Outgoing wave conditions prescribe one solution of each $k, -k$ pair if k is real, and boundedness determines one of the k, k^* pair if k is complex. The number of constraints from both boundaries then equals the number of independent wave solutions.

For complex wave numbers we allow only convergent solutions satisfying $x \text{Im}(k) > 0$. In the Hermitian case these convergent waves do not transport wave energy at infinity. For real wave numbers we define the group velocity v_{gr} , the wave energy W and the energy flow J by the expressions,

$$v_{gr} = \frac{\partial \omega}{\partial k} = - \frac{\Lambda_{,k}}{\Lambda_{,\omega}} \quad (31)$$

$$W = \mathbf{E}^* \cdot \mathbf{D}_{,\omega} \cdot \mathbf{E} \quad , \quad J = - \mathbf{E}^* \cdot \mathbf{D}_{,k} \cdot \mathbf{E}$$

Asymptotically J is conserved for each wave and obeys the familiar relation $J = v_{gr} W$ as follows also from Eqs. (10) and (11). Boundary conditions are assumed for incoming waves, which have group velocities satisfying $x v_{gr} < 0$. The group velocity and the phase velocity $v_{ph} = \omega/k$ are related by ,

$$v_{gr} v_{ph} = -\frac{\omega}{k} \frac{\Lambda_{,k}}{\Lambda_{,\omega}} = -\frac{\Lambda_{,k}^2}{\Lambda_{,\omega}^2} \quad (32)$$

where Λ is a function of k^2 and ω^2 . The waves with opposite wave numbers always have opposite group velocities, but can in general be forward waves, if the r.h.s. is positive, or backward waves, if the r.h.s. is negative.

Let us now assume, that the region $x \rightarrow -\infty$ supports one incoming wave ($v_{gr} > 0$) and N outgoing waves ($v_{gr} < 0$) and the region $x \rightarrow \infty$ M outgoing waves ($v_{gr} > 0$). Global energy conservation requires that

$$J_i + \sum_{n=1}^N J_{rn} = \sum_{m=1}^M J_{tm} \quad (33)$$

where the indices i, r, t denote incident, reflected and transmitted waves, respectively. Defining mode coupling coefficients $R_n = |J_{rn}/J_i|$ for the reflected waves and $T_m = |J_{tm}/J_i|$ for the transmitted waves, one can rewrite Eq.(33) in the form,

$$\sum_{n=1}^N \sigma_n R_n + \sum_{m=1}^M \sigma_m T_m = 1. \quad (34)$$

The sign of each term $\sigma_k = \text{sgn}(W_k/W_i)$ is defined by the sign of the ratio of the wave energies W_k and W_i . Some of the σ_k can be negative, if negative energy waves occur. We also remark, that the coupling coefficients R_n and T_m depend in general both on the wave amplitudes and the group velocities.

We now wish to specify the direction of wave energy flow along spatially disconnected branches. For this purpose we insert the wave representation (10),(11) into the energy flow expression (31) and after using $\sum_j D_{ij} C_{jf} = \Lambda \delta_{if}$, obtain

$$J = -D_{,k} |E_f|^2 \quad (35)$$

In Eq. (35) the energy flow is expressed by the amplitude of the single component E_f and by the function $D(x, k) = \Lambda(x, k)/C_{ff}(x, k)$. This function is well defined for real x and k and is zero along a branch $k = k(x)$. If, as shown in Fig. 2 (where the solid curves plot $k(x)$ for real x), $D > 0$ in the shaded region below one particular curve and $D < 0$ in the unshaded region above that curve then the wave propagation is positive and in the opposite case negative. To determine the sign of J relative to the incident branch, it suffices to draw the contour lines $\Lambda(x, k) = 0$ and $C_{ff}(x, k) = 0$ in the (x, k) -plane, and to observe a sign change of $D(x, k)$ for each crossing of these contour lines. This graphical procedure is illustrated in Fig. 2 by two examples. The solid curves are where $\Lambda(x, k) = 0$, and therefore is the function of $k(x)$. The dashed curve corresponds to where $C_{ff}(x, k) = 0$. These examples show how a sign change of the cofactor C_{ff} inside a tunneling region modifies how one determines the direction of wave propagation on the disconnected branches. Note that C_{ff} is nonzero for scalar wave equations but a sign change can occur for vector systems.

To see how to determine the relative direction of waves when $D(x, k) > 0$ in the shaded regions let us consider Figs. 2a and 2b in more detail. In Fig. 2a let k_c and k_d correspond to waves that propagate to the right and left, respectively as $D_{,k} < 0$ on the “c” branch and greater than zero on the “d” branch. From the topology it is then clear that $D_{,k} < 0$ on the “a” branch and $D_{,k} > 0$ on the “b” branch, hence k_a and k_b correspond to waves propagating to the right and left, respectively. On the other hand in Fig. 2b, if k_c is a right-going wave, and k_d is a left-going wave, then k_a would be a left-going wave and k_b a right-going wave. It is the presence of a zero in C_{ff} that allows for this change of propagation ordering. Note, that in scalar wave equations, where $C_{ff} = 1$, k_a and k_b would have to correspond to right and left-going waves, respectively. Thus, the understanding of the structure of the cofactor is crucial to interpreting the relative propagation directions in regions separated by a tunneling structure.

We now return attention to energy conservation in the WKB framework. For this purpose we propagate a general solution around a branch-point and compare the asymptotic energy flow on both sides. Inside the tunneling region pairs of wave solutions E_f^+ , E_f^- with complex conjugate wave numbers k^+ , k^- give rise to an energy flow,⁶

$$J = - \left[D_{k^+} (E_f^-)^* E_f^+ + \text{c.c.} \right] , \quad (36)$$

where c.c. denotes the complex conjugate expression. Equation (36) generalizes the expression (35) for real wave numbers to the complex case. It should however be noticed, that both asymptotic results are valid in disconnected regions separated by the branch points where k^+ and k^- coalesce. Since the energy flow (36) couples only complex conjugate branches, we consider first a single real branch-point k_B as in Fig. 3a and then a pair of complex conjugate branch-points k_B and k_B^* on the imaginary axis corresponding to a point x_B (as in Fig. 3b).

For real branch-points k_B two propagating waves undergo tunneling. We denote by a^\pm the real branches with $\text{Re}(\delta k) > 0$ for $x > x_B$, and by b^\pm the complex branches with $\text{Im}(\delta k) > 0$ for $x < x_B$, respectively. The corresponding wave solutions for the component E_f are analogously written as A^\pm and B^\pm . Using Eqs.(35) and (36) the energy flows on both sides of x_B can be expressed in the form,

$$\begin{aligned} J(x > x_B) &= - \left[D_{a^+} |A^+|^2 + D_{a^-} |A^-|^2 \right] \\ J(x < x_B) &= - \left[D_{b^+} B^+(B^-)^* + \text{c.c.} \right] \end{aligned} \quad (37)$$

We now propagate the waves A^\pm to the region $x < x_B$ on the path shown in Fig.1 and obtain for the subsequent Stokes' lines S_1 and S_2 the connection formulae,

$$\begin{aligned}
A^-(\rightarrow \bullet) + A^+(\bullet \leftarrow) &\xrightarrow{S_1} A^-(\nwarrow \bullet + \nearrow \bullet) + A^+(\bullet \swarrow) \\
&\xrightarrow{S_2} A^+(\bullet \swarrow + \frac{1}{2} \bullet \searrow) + A^-(\nwarrow \bullet + \nearrow \bullet + \frac{1}{2} \bullet \searrow) \\
&= A^+(\bullet \swarrow + \frac{1}{2} \bullet \searrow) + A^-(\nwarrow \bullet + \frac{1}{2} \nearrow \bullet)
\end{aligned} \tag{38}$$

The solutions B^\pm in the tunneling region are given by the transformation

$$\begin{pmatrix} B^+ \\ B^- \end{pmatrix} = \begin{pmatrix} \bullet \swarrow & \nwarrow \bullet \\ \frac{1}{2} \bullet \searrow & \frac{1}{2} \nearrow \bullet \end{pmatrix} \begin{pmatrix} A^+ \\ A^- \end{pmatrix} \tag{39}$$

Noting, that the complex conjugate diagrams are obtained by reflection about the imaginary axis (Eq. (23)), one finds with Eq. (39),

$$\begin{aligned}
2B^+(B^-)^* &= \begin{array}{c} \bullet \searrow \\ \hline \bullet \swarrow \end{array} |A^+|^2 + \begin{array}{c} \nwarrow \bullet \\ \hline \nearrow \bullet \end{array} |A^-|^2 \\
&+ \begin{array}{c} \bullet \swarrow \\ \hline \bullet \searrow \end{array} A^+(A^-)^* + \begin{array}{c} \nwarrow \bullet \\ \hline \nearrow \bullet \end{array} A^-(A^+)^*
\end{aligned} \tag{40}$$

We now use Eq.(20) to obtain,

$$\begin{array}{c} \text{---} \bullet \text{---} \text{---} \bullet \text{---} \\ \downarrow \quad \uparrow \end{array} = \frac{D_{,a^+}}{D_{,b^+}} \quad , \quad \begin{array}{c} \text{---} \bullet \text{---} \text{---} \bullet \text{---} \\ \downarrow \quad \uparrow \end{array} = \frac{D_{,a^-}}{D_{,b^+}} \quad ,$$

(41)

$$\begin{array}{c} \text{---} \bullet \text{---} \text{---} \bullet \text{---} \\ \downarrow \quad \uparrow \end{array} = - \frac{D_{,b^-}}{D_{,b^+}} \left(\begin{array}{c} \text{---} \bullet \text{---} \text{---} \bullet \text{---} \\ \downarrow \quad \uparrow \end{array} \right)^*$$

From Eqs.(37),(40) and (41) it follows, that $J(x > x_B) = J(x < x_B)$. We have thus obtained energy conservation for branch-points on the real axis.

Next, we consider a pair of complex conjugate branch-points on the imaginary axis and choose an analogous notation (Fig. 3b). In this case the waves are tunneling on both sides of x_B and the corresponding energy flows are,

$$\begin{aligned} J(x > x_B) &= - \left[D_{,a^+} A^+ (C^+)^* + D_{,a^-} A^- (C^-)^* + \text{c.c.} \right] \\ J(x < x_B) &= - \left[D_{,b^+} B^+ (D^-)^* + D_{,b^-} B^- (D^+)^* + \text{c.c.} \right]. \end{aligned} \quad (42)$$

The waves B^\pm are related to the waves A^\pm by Eq.(39) with the branch-point taken in the upper half-plane. Similarly the waves D^\pm are related to the waves C^\pm by choosing the branch-point in the lower half-plane. Evaluating the products in Eq.(42) one finds,

$$\begin{aligned}
2B^+D^{-*} &= \begin{array}{c} \uparrow \\ \cdot \\ \downarrow \end{array} A^+C^{+*} + \begin{array}{c} \uparrow \\ \cdot \\ \downarrow \end{array} A^-C^{-*} + \\
&+ \begin{array}{c} \uparrow \\ \cdot \\ \downarrow \end{array} A^+C^{-*} + \begin{array}{c} \uparrow \\ \cdot \\ \downarrow \end{array} A^-C^{+*} \\
2B^-D^{+*} &= \begin{array}{c} \downarrow \\ \cdot \\ \uparrow \end{array} A^+C^{+*} + \begin{array}{c} \downarrow \\ \cdot \\ \uparrow \end{array} A^-C^{-*} + \\
&+ \begin{array}{c} \downarrow \\ \cdot \\ \uparrow \end{array} A^+C^{-*} + \begin{array}{c} \downarrow \\ \cdot \\ \uparrow \end{array} A^-C^{+*}
\end{aligned} \tag{43}$$

The diagrams in the last line can be written as,

$$\begin{array}{c} \downarrow \\ \cdot \\ \uparrow \end{array} = - \begin{array}{c} \uparrow \\ \cdot \\ \downarrow \end{array} ; \quad \begin{array}{c} \downarrow \\ \cdot \\ \uparrow \end{array} = - \begin{array}{c} \uparrow \\ \cdot \\ \downarrow \end{array}$$
(44)

which leads to cancelation of the corresponding terms in the first product. The remaining diagrams can be combined to the expression for $J(x > x_B)$ by using the identities,

$$\begin{aligned}
\begin{array}{c} \uparrow \\ \cdot \\ \downarrow \end{array} &= \frac{D_{,a^+}}{D_{,b^+}} , & \begin{array}{c} \uparrow \\ \cdot \\ \downarrow \end{array} &= \frac{D_{,a^-}}{D_{,b^+}} \\
\begin{array}{c} \downarrow \\ \cdot \\ \uparrow \end{array} &= \frac{D_{,a^+}}{D_{,b^-}} , & \begin{array}{c} \downarrow \\ \cdot \\ \uparrow \end{array} &= \frac{D_{,a^-}}{D_{,b^-}}
\end{aligned} \tag{45}$$

These results demonstrate energy conservation of the modified Furry rules for any combination of branch-points on the real and imaginary k axis and thereby generalize the discussion of Heading for branch-points at the origin ($k_B = 0$).¹⁸

3 Tunneling with $k_B = 0$

We now apply the WKB method to the most common tunneling problem, which consists of two cut-off points ($k_B = 0$) and a negative branch of k^2 inside the tunneling region. Tunneling in this case is analogous to the quantum-mechanical penetration of a potential barrier. We derive the general connection formula graphically and make comparison with an exact solution for second order equations with a parabolic profile.

A Graphical solution

We consider the tunneling region of Fig.4 with branch-points of $k=k(x)$ at $k=0$, $x=x_{1,2}$ and of $x=x(k)$ at $x=x_0$, $k= \pm ik_0$. For definiteness we will assume, that the k^2 branch describes forward waves with positive wave energy. We propagate the transmitted wave ($k>0$, $x>x_2$) back to the region $x < x_1$ along the path indicated in Fig.4(c). The asymptotic representation is changed, whenever a dominant wave crosses, follows or leaves a Stokes' line. The transmitted wave becomes subdominant on S_1 and on the subsequent lines S_2 , S_3 , S_4 the following waves are induced,

$$\begin{aligned}
 & \bullet \leftarrow \xrightarrow{S_2} \begin{array}{c} \nearrow \\ \bullet \end{array} + \frac{1}{2} \begin{array}{c} \searrow \\ \bullet \end{array} \\
 & \xrightarrow{S_3} \frac{1}{2} \begin{array}{c} \nearrow \\ \bullet \\ \textcircled{x} \end{array} + \left(1 - \frac{1}{4}q\right) \begin{array}{c} \textcircled{x} \\ \downarrow \\ \bullet \end{array} \\
 & \xrightarrow{S_4} \left(1 + \frac{1}{4}q\right) \begin{array}{c} \textcircled{x} \\ \downarrow \\ \bullet \end{array} + \left(1 - \frac{1}{4}q\right) \begin{array}{c} \textcircled{x} \\ \downarrow \\ \bullet \end{array}
 \end{aligned} \tag{46}$$

where

$$q = \begin{array}{c} \textcircled{x} \\ \downarrow \\ \bullet \\ \uparrow \\ \textcircled{x} \end{array} = e^{i\oint k dz}$$

the inner arc corresponding to x_2 and the outer one to x_1 . The last line of Eq.(46) shows the diagrams for the incident and reflected waves in the region $x < x_1$. Dividing by the incident wave one obtains the connection formula,

$$1 + \frac{1 - \frac{q}{4}}{1 + \frac{q}{4}} \begin{array}{c} \curvearrowright \\ \bullet \end{array} \longrightarrow \frac{\begin{array}{c} \textcircled{x} \\ \downarrow \\ \bullet \end{array}}{1 + \frac{q}{4}} \tag{47}$$

We now use Eq.(23) to obtain,

$$\begin{aligned}
 \left| \begin{array}{c} \curvearrowright \\ \bullet \end{array} \right|^2 &= \begin{array}{c} \bullet \\ \curvearrowleft \end{array} \begin{array}{c} \bullet \\ \curvearrowright \end{array} = - \frac{D_{,k_i}}{D_{,k_r}} \\
 \left| \begin{array}{c} \textcircled{x} \\ \downarrow \\ \bullet \end{array} \right|^2 &= \begin{array}{c} \textcircled{x} \\ \downarrow \\ \bullet \\ \uparrow \\ \textcircled{x} \end{array} \begin{array}{c} \textcircled{x} \\ \downarrow \\ \bullet \\ \uparrow \\ \textcircled{x} \end{array} = q \frac{D_{,k_i}}{D_{,k_t}}
 \end{aligned} \tag{48}$$

The reflection and transmission coefficients as defined by Eq.(34) can then be written in the form,

$$R = \frac{\left(1 - \frac{q}{4}\right)^2}{\left(1 + \frac{q}{4}\right)^2} ; \quad T = \frac{|q|}{\left(1 + \frac{q}{4}\right)^2} . \quad (49)$$

In the expression for T we have taken the magnitude of q to allow for later generalizations, where q may become negative. It is readily seen, that this result obeys energy conservation in the form $R + T = 1$.

We finally note, that the cofactor C_{ff} cannot change sign in the present case, where k^2 is taken real. Here \mathbf{D} is Hermitian and has real eigenvalues λ_n and orthonormal eigenvectors \mathbf{e}_n , satisfying the relation,

$$\mathbf{D} \cdot \mathbf{e}_n = \lambda_n \mathbf{e}_n , \quad (50)$$

locally. Along the chosen branch we may set $\lambda_1 = 0$, $\mathbf{E} = a\mathbf{e}_1$, $\lambda_2 \neq 0$, $\lambda_3 \neq 0$ to obtain,

$$\mathbf{E}^* \cdot \mathbf{D} \cdot \mathbf{E} = \frac{\Lambda}{C_{ff}} |\mathbf{E}_f|^2 = \lambda_1 |a|^2 . \quad (51)$$

With $\Lambda = \lambda_1 \lambda_2 \lambda_3$ the cofactor C_{ff} can be expressed as,

$$C_{ff} = \lambda_2 \lambda_3 |\mathbf{E}_f|^2 / |a|^2 . \quad (52)$$

It follows, that C_{ff} is non-zero under the assumptions made. If k^2 becomes complex \mathbf{D} is generally no longer Hermitian and then this argument fails.

B Model equation

As an example for wave tunneling with $k^2 < 0$ we consider a second order equation with a parabolic profile,

$$\Psi''(x) + \left(\frac{1}{4} x^2 - a \right) \Psi(x) = 0 \quad (53)$$

with a constant $a > 0$. We specialize the general solution to the present case by setting,

$$E_f = \Psi, \quad C_{ff} = 1, \quad \Lambda = -k^2 + \frac{x^2}{4} - a. \quad (54)$$

To evaluate the diagrams for the wave amplitudes it is convenient to define the branches of $\Lambda(z,k) = 0$ in the form,

$$z = 2\sqrt{a} \cosh(\tau), \quad k = -\sqrt{a} \sinh(\tau). \quad (55)$$

This is a particular solution of Eq.(6), that corresponds to the initial conditions $z(0)=2\sqrt{a}$, $k(0) = 0$ at $\tau = 0$. The mapping (55) is 2π -periodic along the imaginary τ axis, and one can therefore restrict attention to the strip $-\pi < \text{Im}(\tau) < \pi$. Some values of (z,k) assumed at representative points are shown in Fig.5

The τ representation of the path becomes especially convenient for the loop diagram q . Here the integration path, connecting the points $(-2\sqrt{a}, 0)$, $(0, i\sqrt{a})$, $(2\sqrt{a}, 0)$, $(0, -i\sqrt{a})$, is mapped in the τ -plane on the imaginary axis from $-\pi$ to $i\pi$. Noting that,

$$\int k dz = \int k(\tau) \frac{dz(\tau)}{d\tau} d\tau = a \left[\tau - \frac{1}{2} \sinh(2\tau) \right], \quad (56)$$

$$\oint k dz = 2\pi i a,$$

one finds,

$$q = e^{i \oint k dz} = e^{-2\pi a}. \quad (57)$$

Using for the reflected wave the relations $a(k|1,2) = 1$, $\delta(k|1,2) = \pi$ and for the transmitted waves the relations $a(k|1,2) = \sqrt{k_1/k_2}$, $\delta(k|1,2) = 0$, one obtains the expressions,

$$\begin{array}{c} \curvearrowright \\ 2 \end{array} \begin{array}{c} \bullet \\ | \end{array} = -i e^{2iS_1}$$

(58)

$$\begin{array}{c} \textcircled{x} \\ | \\ \bullet \end{array} \begin{array}{c} | \\ \curvearrowright \\ 2 \end{array} = \sqrt{\frac{k_1}{k_2}} e^{-\pi a} e^{i(S_1 + S_2)}$$

where,

$$S_1 = - \int_{-2\sqrt{a}}^{x_1} \left(\frac{x^2}{4} - a \right)^{1/2} dx, \quad S_2 = \int_{2\sqrt{a}}^{x_2} \left(\frac{x^2}{4} - a \right)^{1/2} dx.$$

The WKB connection formula (47) then assumes the form,

$$1 - i \frac{1 - \frac{1}{4} e^{-2\pi a}}{1 + \frac{1}{4} e^{-2\pi a}} e^{2iS_1} \longrightarrow \frac{e^{-\pi a}}{1 + \frac{1}{4} e^{-2\pi a}} \sqrt{\frac{k_1}{k_2}} e^{i(S_1 + S_2)} \quad (59)$$

The exact solution of the present boundary value problem is given by the parabolic cylinder function $E(a, x)$.²¹ Using Darwin's expansion, the exact connection formula follows to be,

$$1 - i \frac{1}{\sqrt{1 + e^{-2\pi a}}} e^{2iS_1} \longrightarrow \frac{e^{-\pi a}}{\sqrt{1 + e^{-2\pi a}}} \sqrt{\frac{k_1}{k_2}} e^{i(S_1 + S_2)} \quad (60)$$

Both results conserve wave energy, predict the same phases and are in agreement up to the order $e^{-2\pi a}$. This accuracy could not have been obtained by using the usual Furry rules.

4 Tunneling with $k_B > 0$

We now treat tunneling with a non-zero real part of k and branch-points $k_B > 0$. In contrast to the previous case the orientation of the energy flow now depends on the special form of the cofactors.

A Graphical solution

Let us construct the global solution for the tunneling structure of Fig.6. Here couplings occur between branches of the same sign, which we take to be positive. The branch-points are denoted as x_1, k_1 and x_2, k_2 . We identify the incoming wave with the upper k -branch in the region $x < x_1$ and assume first, that the transmitted wave is given by the lower k -branch in the region $x > x_2$. Analogously to the procedure in Sec.3 we propagate the transmitted wave back to the region $x < x_1$ and obtain there the asymptotic representation,

$$\begin{array}{c} \text{---} \bullet \xrightarrow{\quad} \text{---} \bullet \end{array} \left(1 + \frac{1}{4}q\right) + \begin{array}{c} \text{---} \bullet \xleftarrow{\quad} \text{---} \bullet \end{array} \left(1 - \frac{1}{4}q\right) \quad (61)$$

with

$$q = \begin{array}{c} \text{---} \bullet \xrightarrow{\quad} \text{---} \bullet \\ \text{---} \bullet \xleftarrow{\quad} \text{---} \bullet \end{array} = \sigma e^{i \oint k dz}$$

$$\sigma = \text{sgn} \left(\frac{W_t}{W_i} \right).$$

It has the same form as in Eq. (46), and therefore the mode coupling coefficients are still given by the expressions (49), however with q as defined in Eq. (61). The conservation relation now assumes the general form $R + \sigma T = 1$. If σ is negative, the reflection coefficient becomes larger than 1.

In the case, where the transmitted wave is given by the upper k -branch, energy conservation is obtained in exactly the same manner. It follows from Eq.(39), that all diagrams are only changed at the arcs around k_2 . Accordingly, the contour in the q diagram passes around k_2 on the opposite side, leading to the same expression for σ .

B Model system

The coupling between crossing branches can often be described by a matrix,¹²

$$D_{ij} = \begin{bmatrix} a(x,k) & ic \\ -ic^* & b(x,k) \end{bmatrix}, \quad (62)$$

where c denotes a small coupling constant and the functions $a(x,k)$, $b(x,k)$ have a common zero at x_0 , k_0 . Expanding about the crossing point x_0 , k_0 up to linear terms and setting $\Lambda(x,k) = 0$, one obtains,

$$\tilde{k}_{1,2} = \frac{-B_{\pm} \tilde{x} \pm (B_{\pm}^2 \tilde{x}^2 - 4A|c|^2)^{1/2}}{2A}, \quad (63)$$

with $\tilde{k} = k - k_0$, $\tilde{x} = x - x_0$, $A = a_k b_k$ and $B_{\pm} = a_x b_k \pm a_k b_x$. Tunneling occurs if $A > 0$, yielding for the branch-points \tilde{x}_B and the maximum imaginary part of the wave number k_m the expressions,

$$\tilde{x}_B = \pm 2|c| \sqrt{A} / |B_{\pm}|, \quad k_m = |c| / \sqrt{A}. \quad (64)$$

The integral around the branch-points, that determines the transmission coefficient then follows to be,

$$\oint k dz = \pi k_m |\tilde{x}_B| = 2\pi \frac{|c|^2}{|B_{\pm}|}. \quad (65)$$

This expression agrees with previous results for coupled differential equations.¹²

We now discuss the role of the cofactors in this model. From Eqs.(11) and (62) the matrix of the cofactors follows to be,

$$C_{ij} = \begin{bmatrix} b(x,k) & -ic \\ ic^* & a(x,k) \end{bmatrix} \quad (66)$$

According to the discussion of Eq.(35) the energy flow direction is determined by the zeros of one of the cofactors C_{11} or C_{22} . The equations $C_{11} = 0$, $C_{22} = 0$ describe two straight lines, forming asymptotes to the branches for $|\tilde{x}_B| \rightarrow \infty$ and intersecting inside the tunneling region at the crossing point. The corresponding energy flow direction is given by Fig.2(b).

Outside the tunneling region the asymptotic solution can be written in the form,

$$\begin{bmatrix} E_1 \\ E_2 \end{bmatrix} = \begin{bmatrix} 1 \\ \frac{C_{21}}{C_{11}} \end{bmatrix} \bigg|_{a=0} \Psi_1 + \begin{bmatrix} \frac{C_{12}}{C_{22}} \\ 1 \end{bmatrix} \bigg|_{b=0} \Psi_2, \quad (67)$$

where the waves Ψ_1 and Ψ_2 correspond to the branches $a=0$ and $b=0$, respectively. The polarization ratios, entering this expression, are given by

$$\frac{C_{12}}{C_{22}} \bigg|_{b=0} = \frac{-icb_{,k}}{B_- \tilde{x}}, \quad \frac{C_{21}}{C_{11}} \bigg|_{a=0} = \frac{-ic^*a_{,k}}{B_- \tilde{x}} \quad (68)$$

They have apparently first been noted in Ref.12, by iteratively solving a system of coupled wave equations. Our treatment shows, that these factors arise naturally from the WKB theory of vector systems.

5 Four-wave tunneling problems

In the presence of additional branch-points, more than two waves can be coupled in a tunneling process. We now discuss two examples, which are commonly encountered in four-wave interactions.

A Exterior cut-off

Suppose we have the configuration of Fig. 7 with branch-points at $(x_0, 0)$, $(x_1, \pm k_1)$ and $(x_2, \pm k_2)$. The positive and negative branches are connected by the cut-off at x_0 . In the region $x < x_0$ we assume an incoming wave with $k > 0$ and demand, that no growing waves exist with $\text{Im}(k) > 0$. In the region $x > x_2$ the transmitted waves are taken on the lower k -branches.

Let us first construct the particular solution, where only one transmitted wave ($k > 0$) is present. For this wave the asymptotic representation in the region $x_0 < x < x_1$ is given by Eq.(61). Propagating this solution further into the region $x < x_0$ only the outgoing wave proceeds to the cut-off and induces another wave on S_6 . For $x < x_0$ the asymptotic solution then follows to be,

$$\left(1 + \frac{q}{4}\right) \cdot \text{diagram}_1 + \left(1 - \frac{q}{4}\right) \left(\text{diagram}_2 + \frac{1}{2} \text{diagram}_3 \right) \quad (69)$$




where q is given by Eq.(61) and the $+$ sign indicates, that the branch-points are taken on the positive k axis. The transmitted wave with $k < 0$ for $x > x_2$ leads analogously to the representation,

$$\left(1 - \frac{q}{4}\right) \cdot \text{diagram}_4 + \left(1 + \frac{q}{4}\right) \left(\text{diagram}_5 + \frac{1}{2} \text{diagram}_6 \right) \quad (70)$$




with the branch-points taken on the negative k axis. We also have used Eq.(20) to obtain the identity,

$$\text{Loop}(-) = \text{Loop}(-) + \text{Loop}(+) \circ \text{Loop}(+) = q \quad (71)$$

We now combine both particular solutions such, that the growing waves with $\text{Im}(k) > 0$ cancel. This can be achieved, by adding to the first solution the second one multiplied by the factor,

$$\text{Sequence of loops} \cdot r = \frac{1 - \frac{q}{4}}{1 + \frac{q}{4}} \quad (72)$$

Dividing the result by the incident wave yields the connection formula,

$$\begin{aligned} & 1 + \text{Sequence of loops} \cdot r^2 + \text{Sequence of loops} \cdot r \\ & \rightarrow \frac{\text{Loop}(+)}{1 + \frac{q}{4}} + r \cdot \text{Sequence of loops} \cdot \frac{\text{Loop}(-)}{1 + \frac{q}{4}} \end{aligned} \quad (73)$$

The transmission coefficients T_1 and T_2 for the waves with $k > 0$ and $k < 0$, respectively and the reflection coefficient R then are found to be,

$$T_1 = \frac{|q|}{(1 + q/4)^2},$$

$$T_2 = r^2 T_1 = T_1 (1 - T_1), \quad (74)$$

$$R = r^4 = (1 - T_1)^2.$$

Energy conservation holds again in the form, $R + \sigma(T_1 + T_2) = 1$. This result is consistent with the physical consideration, that from the incident power a fraction T_1 is transmitted to the first wave and a fraction $1 - T_1$ reflected to the cut-off. The latter energy flux can transmit a fraction $T_1(1 - T_1)$ to the second wave, while a fraction $(1 - T_1)^2$ remains for the reflected wave.

B Interior complex branch-point

We now analyse the case, where the incident wave reaches first the cut-off and then tunnels to an additional complex branch-point (Fig.8). We assume the same boundary and outgoing wave conditions as before and first derive the solution corresponding to a single transmitted wave. The transmitted wave with $k > 0$ induces up to S_4 the following waves,

$$\begin{aligned}
 & \bullet \rightarrow \bullet \xrightarrow{S_1} \text{diagram 1} + \text{diagram 2} \xrightarrow{S_2} \text{diagram 3} + \frac{1}{2} \text{diagram 4} \\
 & \xrightarrow{S_4} \frac{1}{2} \text{diagram 5} + \frac{1}{2} \text{diagram 6} + \text{diagram 7} + \frac{1}{4} \text{diagram 8}
 \end{aligned} \quad (75)$$

It is noted, that on S_3 both waves have $\text{Im}(\delta k) > 0$ and are therefore subdominant. Proceeding to the region $x < x_0$ only the first two diagrams induce further waves. Their continuation yields,

$$\frac{1}{2} \begin{array}{c} \bullet \\ \uparrow \\ \bullet \end{array} \begin{array}{c} \bullet \\ \downarrow \\ \bullet \end{array} + \frac{1}{2} \begin{array}{c} \bullet \\ \downarrow \\ \bullet \end{array} \begin{array}{c} \bullet \\ \uparrow \\ \bullet \end{array}$$

$$\xrightarrow{S_5} \frac{1}{2} \begin{array}{c} \bullet \\ \uparrow \\ \bullet \end{array} \begin{array}{c} \bullet \\ \downarrow \\ \bullet \end{array} + \frac{1}{2} \begin{array}{c} \bullet \\ \downarrow \\ \bullet \end{array} \begin{array}{c} \bullet \\ \uparrow \\ \bullet \end{array} (1 - \frac{1}{2} q) \quad (76)$$

$$\xrightarrow{S_6} \frac{1}{2} \begin{array}{c} \bullet \\ \downarrow \\ \bullet \end{array} \begin{array}{c} \bullet \\ \uparrow \\ \bullet \end{array} (1 - \frac{q}{2}) + \frac{1}{2} \begin{array}{c} \bullet \\ \uparrow \\ \bullet \end{array} \begin{array}{c} \bullet \\ \downarrow \\ \bullet \end{array} (1 + \frac{q}{2})$$

with

$$q = \begin{array}{c} \bullet \\ \downarrow \\ \bullet \end{array} \begin{array}{c} \bullet \\ \uparrow \\ \bullet \end{array} = \sigma e^{i\phi k dz} \quad (77)$$

and $\sigma = \text{sgn}(W_t/W_i)$. The second transmitted wave with $k < 0$ similarly leads to the two tunneling waves,

$$\begin{array}{c} \bullet \\ \downarrow \\ \bullet \end{array} \begin{array}{c} \bullet \\ \uparrow \\ \bullet \end{array} + \frac{1}{4} \begin{array}{c} \bullet \\ \downarrow \\ \bullet \end{array} \begin{array}{c} \bullet \\ \uparrow \\ \bullet \end{array} \quad (78)$$

and to the two propagating waves,

$$\frac{1}{2} \begin{array}{c} \bullet \\ \downarrow \\ \bullet \end{array} \begin{array}{c} \bullet \\ \uparrow \\ \bullet \end{array} (1 - \frac{q}{2}) + \frac{1}{2} \begin{array}{c} \bullet \\ \uparrow \\ \bullet \end{array} \begin{array}{c} \bullet \\ \downarrow \\ \bullet \end{array} (1 + \frac{q}{2}) \quad (79)$$

Here we used an identity analogous to Eq.(71). We now multiply the second solution by the factor,

(80)

and add the product to the first solution. Then the tunneling waves vanish identically,

(81)

and from the remaining waves we obtain the connection formula,

$$1 + \frac{1 - \frac{q}{2}}{1 + \frac{q}{2}} \rightarrow \frac{\text{diagram 1}}{1 + \frac{q}{2}} + \frac{\text{diagram 2}}{1 + \frac{q}{2}} \quad (82)$$

The reflection and transmission coefficients now follow to be,

$$R = \frac{(1 - \frac{q}{2})^2}{(1 + \frac{q}{2})^2} ; \quad T_1 = T_2 = \frac{|q|}{(1 + \frac{q}{2})^2} , \quad (83)$$

satisfying the conservation relation $R + \sigma(T_1 + T_2) = 1$.

The tunneling structure with an interior complex branch-point occurs for mode conversion in thermal plasmas for mode conversion between fast Alven waves and ion Bernstein waves at the two-ion hybrid resonance.^{5,7-9} The dielectric tensor near the resonance assumes the approximate form,²²

$$\mathbf{D}_{ij} = \begin{bmatrix} a + \alpha n^2 & b \\ b^* & a - n^2 \end{bmatrix} \quad (84)$$

with,

$$a = 1 - \sum_j \frac{\omega_{pj}^2}{\omega^2 - \omega_{cj}^2}$$

$$b = -i \sum_j \frac{\omega_{cj}}{\omega} \frac{\omega_{pj}^2}{\omega^2 - \omega_{cj}^2}$$

$$\alpha = \sum_j \left(\frac{\omega_{pj}^2}{\omega^2 - \omega_{cj}^2} - \frac{\omega_{pj}^2}{\omega^2 - 4\omega_{cj}^2} \right) \frac{k^2}{\omega_{cj}^2} \frac{T}{m_j}$$

$$n = \frac{c}{\omega} k ,$$

where c denotes the speed of light, T the temperature, ω_p the plasma frequency, ω_c the cyclotron frequency, m the mass and j labels the particle species. From Eq.(84) the dispersion relation $\Lambda = 0$ is obtained as,

$$n^4 + \left(\frac{1}{\alpha} - 1 \right) a n^2 + \frac{1}{\alpha} (|b|^2 - a) = 0 . \quad (85)$$

The branches for the wave numbers are given by,

$$n^2 = -A \pm \sqrt{B} \quad (86)$$

where

$$A = \left(\frac{1}{\alpha} - 1\right) \frac{a}{2}, \quad B = A^2 + \frac{a^2 - |b|^2}{\alpha}.$$

There occurs a cut-off for $a^2 = |b|^2$ and further branch-points at $n^2 = -A$ for $a^2 = 4\alpha|b|^2/(1 + \alpha)^2$. The asymptotic branches are given by, $n^2 = a(1 - |b|^2/a^2)$, for the Alfvén waves and by, $n^2 = -a/\alpha$, for the ion Bernstein waves. Assuming now, that the parameter a varies from positive to negative values along the x -axis, one obtains the general structure of Fig. 8. The contours $C_{ff} = 0$ are also easily obtained from $C_{11} = a - n^2$ and $C_{22} = a + \alpha n^2$. They describe asymptotes to the Alfvén wave branches ($a > 0$) and to the Bernstein wave branches ($a < 0$) that intersect at $a = 0$. The orientation of the energy flow is again given by Fig. 2(b). The imaginary parts of the wave numbers in the two sections of the tunneling region can be expressed as,

$$k_1 = \pm \frac{\omega}{c} \begin{cases} \sqrt{A - \sqrt{B}} & ; B > 0 \\ \sqrt{\frac{A + \sqrt{A^2 + |B|}}{2}} & ; B < 0 \end{cases} \quad (87)$$

These determine the mode coupling coefficients according to Eqs. (77) and (83) for general profiles.

6 Conclusions

Our analysis of wave tunneling has led to transmission coefficients, that are given by loop integrals around the branch-points of the tunneling structure. These integrals are entirely determined by the local dispersion relation and therefore will not depend on the specific operator representation, that has been used. This independence may explain the general agreement of various mode conversion models on the form of the transmission coefficients.⁷⁻¹⁴

The direction of the energy flow depends similarly on the dispersion relation, but generally also on the cofactors of the dielectric tensor. These cofactors describe the vector structure of the wave amplitudes and can lead to a sign change of the energy flow across the tunneling region. The vector representation in the present treatment is therefore appropriate to describe the forward and backward nature of the waves.

Energy conservation in the WKB theory has been obtained by the use of a modified Furry rule. This technique applies to extended tunneling regions, where each branch-point can be treated separately. When this approximation is justified, we can then describe coupling with coalescing branches both on the real and on the imaginary k axis. For non-separable branch-points different WKB techniques have been developed, which are however limited to specific second order equations.^{18,23}

In summary, the present treatment of wave tunneling is based on the general dielectric tensor of the medium, conserves the physical wave energy for dissipationless systems and can be applied to arbitrary mode complexity by following simple graphical rules.

Acknowledgments:

This work was supported by the Deutsche Forschungsgemeinschaft (Bonn,FRG) and by the U.S. Department of Energy , contract No.: DE-FG05-80ET53088.

Appendix: Derivation of Modified Furry Rule

From Eqs. (27) and (28) we have that the solutions for the components of the electric field $E(z)$ are,

$$E_i(z) = \int_C dk \hat{a}_i(k) \exp [ikz - i\hat{S}(k)] \quad (\text{A1})$$

with,

$$\hat{a}_i(k) = \frac{1}{\sqrt{2\pi i}} \left(\frac{C_{if}}{C_{ff}\sqrt{D_{,z}}} \right) \Big|_{z=z(k)}, \quad \hat{S}(k) = \hat{S}(k_T) + \int_{k_T}^k dk' z(k').$$

The reader is reminded, that $z(k)$ is determined from the local dispersion relation $\Lambda(z, k) = 0$ and that $dz/dk = 0$ at the branch-point k_T . Assuming a sufficiently rapidly varying phase, we can approximately evaluate Eq. (A1) by expanding $z(k)$ about k_T . With $z_T = z(k_T)$, $z_T'' = z''(k_T)$, $\delta k = k - k_T$, $\delta z = z - z_T$, the two WKB wavelets that merge at $k = k_T$ can then be accurately described by the integral form,

$$E_i(z) = \exp [ik_T z - \hat{S}(k_T)] \int_C dk \hat{a}_i(k) \exp \left[i\delta z \delta k - i\frac{z_T''}{6} \delta k^3 + \dots \right]. \quad (\text{A2})$$

The k -space integral is basically an Airy integral if the sum is truncated after the cubic term and the amplitude \hat{a}_i is slowly varying.

For the Hermitian problems we are considering, x_T , k_T^2 and consequently also z_T'' are real. For definiteness let us assume $z_T'' > 0$. The stationary phase points are at $\delta k = \pm \sqrt{2\delta z/z_T''}$ and the corresponding solutions are then propagating waves for $\delta z > 0$ and evanescent waves for $\delta z < 0$. The contours of the k -space integration are shown in Fig. 9. In the figure the shaded regions are where the integrand is divergent as $|k - k_T| \rightarrow \infty$. For $\delta z > 0$ the stationary phase points A ($\delta k > 0$) and B ($\delta k < 0$) are shown in Fig. 9a. The solid contour is the steepest descent contour through point A and the dashed contour the steepest descent contour through point B. By choosing one of these contours a single propagating wave with $k(z) = k_T + \delta k$ is obtained.

Let us suppose that the solution of interest for $\delta z > 0$ corresponds to a single WKB wavelet with $\delta k > 0$. The contour of integration is the solid contour in Fig. 9a. For $\delta z < 0$ the stationary phase points are on the imaginary axis. Equivalent to the solid contour in Fig. 9a is the solid contour in Fig. 9b. The new contour goes along the directions of steepest descent through the stationary phase point A', where $\delta k = i\sqrt{2|\delta z|/z_T''} \equiv \delta k_1$, and the stationary phase point B', where $\delta k = -i\sqrt{2|\delta z|/z_T''} \equiv \delta k_2$. In approximating the contour integrals by the steepest descent method, we see that only *one-half* of the saddle point integral through B' is needed.

We now evaluate the saddle point integrals by the method of stationary phase. For $\delta z > 0$ the saddle point contribution from the stationary phase point A is given by,

$$E_i(z) \approx \hat{a}_i \Big|_{k=k(z)} \exp[iS(z)] \int_C dp \exp\left[-\frac{i}{2} z_T'' \delta k p^2\right] \quad (\text{A3})$$

with

$$S(z) = k_T z - \hat{S}(k_T) + \frac{2}{3} \delta z \delta k = S(z_T) + \int_{z_T}^z dz' k(z')$$

and $S(z_T) = z_T k_T - \hat{S}(k_T)$. Defining $\alpha = \arg(i\delta k)$ and $p = te^{i\varphi}$ the directions of steepest descent at the stationary phase point satisfy the condition $\varphi = -\alpha/2 + n\pi$. In accordance with the orientation of the solid contour in Fig. 9a ($\varphi = -\pi/4$) we choose $n = 0$ and find,

$$E_i(z) = \hat{a}_i \Big|_{k=k(z)} e^{iS(z)} \left(\frac{2\pi}{iz_T'' \delta k}\right)^{1/2} = \left(\frac{C_{if}}{C_{ff} i \sqrt{-D_{,k}}}\right) \Big|_{k=k(z)} e^{iS(z)}. \quad (\text{A4})$$

Here the phase of $-D_{,k}$ is determined by the relation, $-D_{,k} = D_{,z} dz(k)/dk = D_{,z} z_T'' \delta k$.

For $\delta z < 0$ there are two saddle points that the contour of integration passes through. The stationary phase contribution through the point A' produces the dominant wavelet and the stationary phase contribution through the point B' one-half of the subdominant wavelet corresponding to a Stokes' factor 1/2. Specifically, the steepest descent evaluations yield,

$$\begin{aligned} E_i(z) &\approx \hat{a}_i \Big|_{k=k_1(z)} e^{iS_1} \frac{(-i)\sqrt{2\pi}}{\sqrt{|iz_T'' \delta k|}} + \frac{1}{2} \hat{a}_i \Big|_{k=k_2(z)} e^{iS_2} \frac{\sqrt{2\pi}}{\sqrt{|iz_T'' \delta k|}} \\ &= \left(\frac{C_{if}}{C_{ff} i \sqrt{-D_{,k}}}\right) \Big|_{k=k_1(z)} e^{iS_1} + \frac{1}{2} \left(\frac{C_{if}}{C_{ff} i \sqrt{-D_{,k}}}\right) \Big|_{k=k_2(z)} e^{iS_1}, \end{aligned} \quad (\text{A5})$$

where $\arg(\delta k_1) = \pi/2$, $\arg(\delta k_2) = -\pi/2$ and the subscripts 1, 2 denote evaluation with $\delta k_{1,2}$, respectively. The dominant wavelet 1 is the analytic continuation in the upper half k -plane of the original WKB wavelet. The subdominant wavelet 2 is the analytic continuation of the wavelet 1 around the branch point in the opposite sense of propagation. This result is just the modified Furry rule given diagrammatically in Eq. (26).

References

1. L.D. Landau, and E.M. Lifshitz: *Quantum Mechanics* (Pergamon Press, New York, 1958).
2. T.H. Stix, and D.G. Swanson: *Handbook of Plasma Physics Vol. 1*, Eds.: M. N. Rosenbluth, and R.Z. Sagdeev (North-Holland Publishing Company, 1983).
3. H.L. Berk, R.R. Dominguez, and E.K. Maschke, *Phys.Fluids* **24**, 2245 (1981).
4. R.R. Dominguez, and H.L. Berk, *Phys. Fluids* **27**, 1142 (1984).
5. P.L. Colestock, and R.J. Kashuba, *Nucl. Fusion* **23**, 763 (1983).
6. H.L. Berk, H.J. Kull, and P.J. Morrison (To be published)
7. D.G. Swanson, *Phys. Rev. Lett.* **36**, 316 (1976).
8. Y.C. Ngan, and D.G. Swanson, *Phys. Fluids* **20**, 1920 (1977).
9. D.G. Swanson, *Phys. Fluids* **28**, 2645 (1985).
10. V. Fuchs, K. Ko, and A. Bers, *Phys. Fluids* **24**, 1251 (1981).
11. V. Fuchs, A. Bers, and L. Harten, *Phys. Fluids* **28**, 177 (1985).
12. R.A. Cairns and C.N. Lashmore-Davies, *Phys. Fluids* **26**, 1268 (1983).
13. L. Friedland, *Phys. Fluids* **29**, 1105 (1986).
14. L. Friedland, G. Goldner and A.N. Kaufman, *Phys, Rev. Lett.* **58**, 1392 (1987).
15. H.L. Berk, and D. Pfirsch, *J. Math. Phys.* **21**, 2054 (1980).
16. H.L. Berk, W.M. Nevins, and K.V. Roberts, *J. Math. Phys.* **23**, 988 (1982).
17. J.B. Keller, *Ann. Phys.* **4**, 180 (1958).
18. J. Heading: *An Introduction to Phase-Integral Methods*, (John Wiley & Sons Inc., New York, 1962).
19. S. Riyopoulos, and T. Tajima, *Phys. Fluids* **29**, 4161 (1986).
20. P. Henrici: *Applied and Computational Complex Analysis* (John Wiley & Sons, New York, 1977).
21. M. Abramowitz, and I.A. Stegun: *Handbook of Mathematical Functions* (Dover Publications , Inc., New York, 1965).
22. V.N. Oraevsky: *Handbook of Plasma Physics Vol. 1*, Eds.: M.N. Rosenbluth, and R.Z. Sagdeev (North-Holland Publishing Company, 1983).
23. F.L. Hinton , *J. Math. Phys.* **20**, 2036 (1979).

Figure Captions

1. Stokes' lines emanating from a branch-point x_B into the complex plane with one line along the real axis. The lines are labeled by the sign of $\text{Im}(\delta k)$ of the dominant wave and the path of wave propagation is indicated.
2. Directions of energy flow. $D(x, k)$ is assumed positive in the shadowed areas and changes sign across the solid contours $\Lambda(x, k) = 0$ (—) and across the dashed contours $C_{ff}(x, k) = 0$ (----).
 - (a) Tunneling region with $C_{ff} \neq 0$.
 - (b) Tunneling region with $C_{ff} = 0$.
3. Branch-points (a) on the real and (b) on the imaginary axis in the k -plane. The notation used for the merging roots is indicated.
4. Potential-barrier model
 - (a) Tunneling region with $k^2 < 0$.
 - (b) Branches of $\Lambda(x, k) = 0$ and energy flow directions.
 - (c) Stokes'-lines.
5. Strip $-\pi < \text{Im}(\tau) < \pi$ of the τ -plane with values of (z, k) at representative points.
6. Tunneling region with real branch-points $k_B \neq 0$.
7. Four wave tunneling problem with an exterior cut-off.
 - (a) Tunneling configuration with an exterior cut-off.
 - (b) Schematic representation of Stokes' lines.
8. Four wave tunneling problem with additional complex branch points.
 - (a) Tunneling configuration with an interior branch-point.
 - (b) Corresponding Stokes'-lines.

9. Local k -space contours in the vicinity of the turning point $k = k_T$. The steepest descent contour when $x - x_T > 0$ shown in (a) goes through the saddle point A and leads to a WKB propagating wave. An equivalent contour when $x - x_T < 0$ has the steepest descent contour going through the saddle points A' and B' and leads to exponentially growing and exponentially decaying waves.

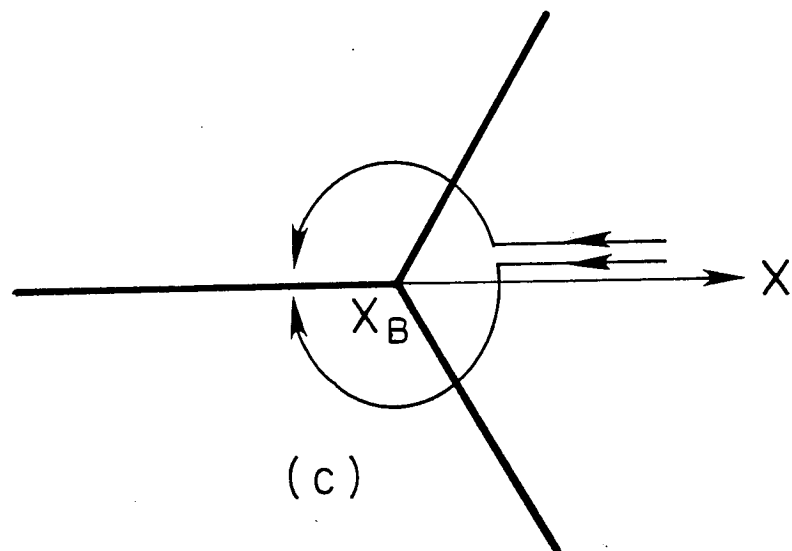
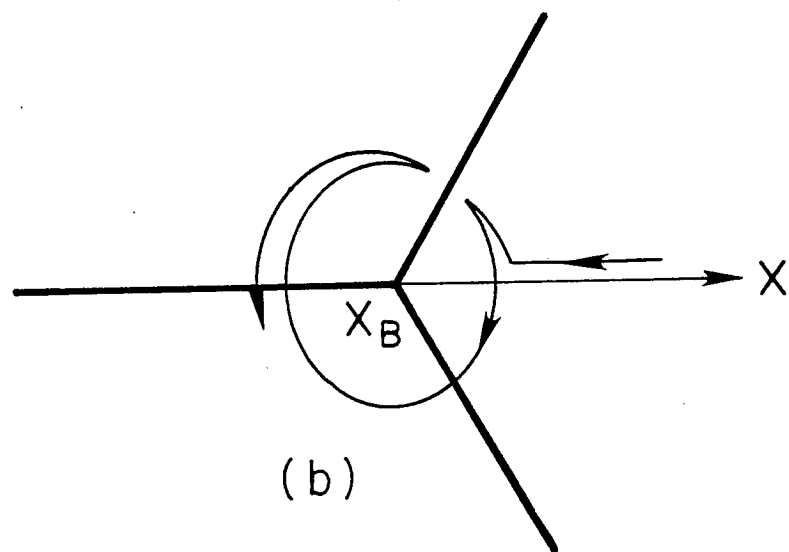
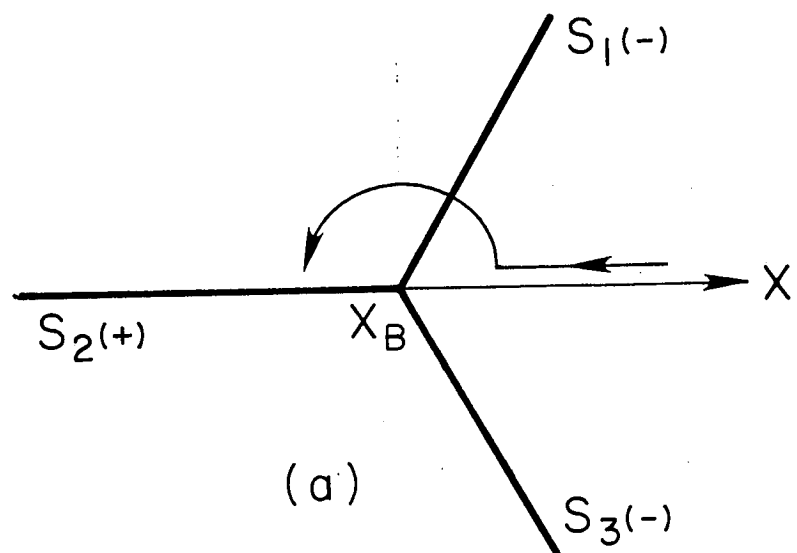


Fig. 1

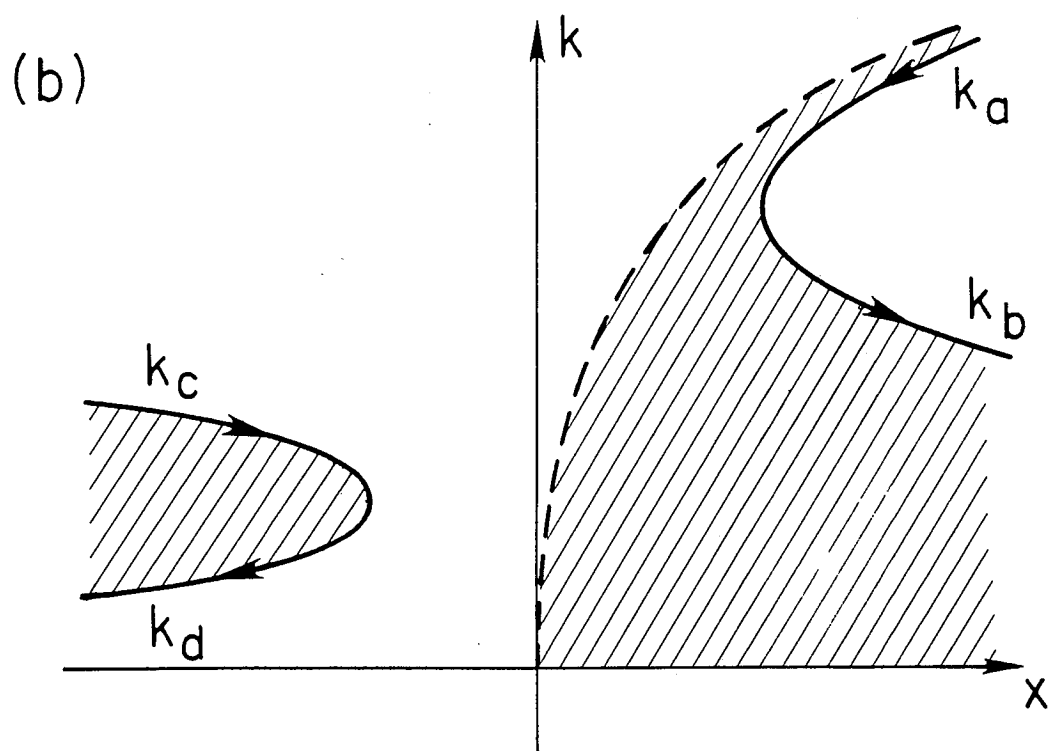
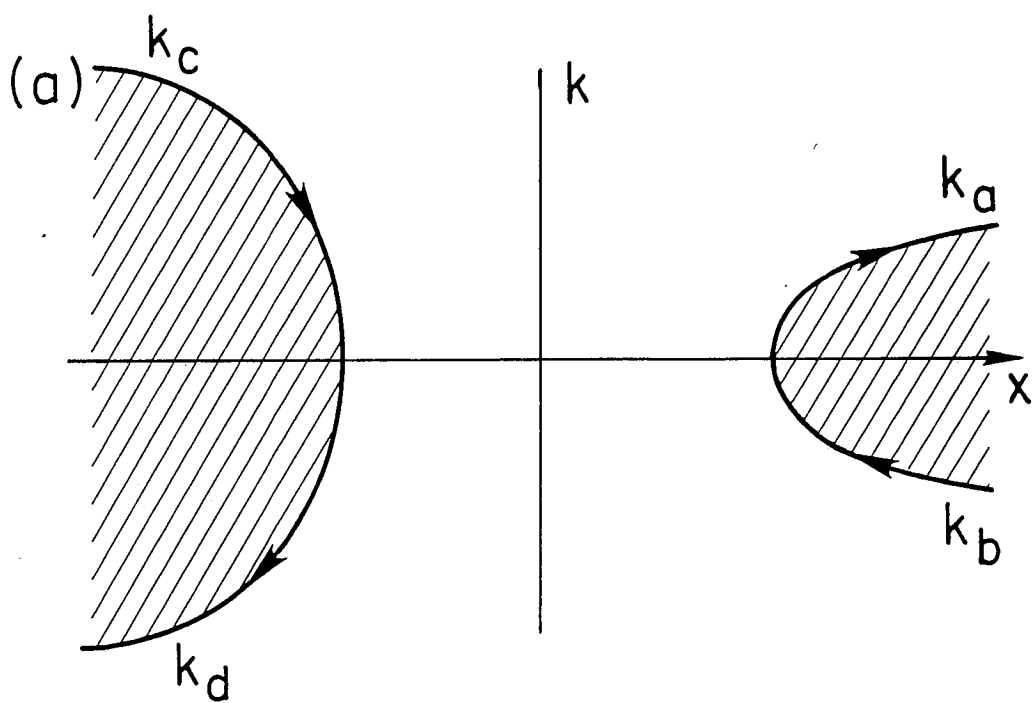


Fig. 2

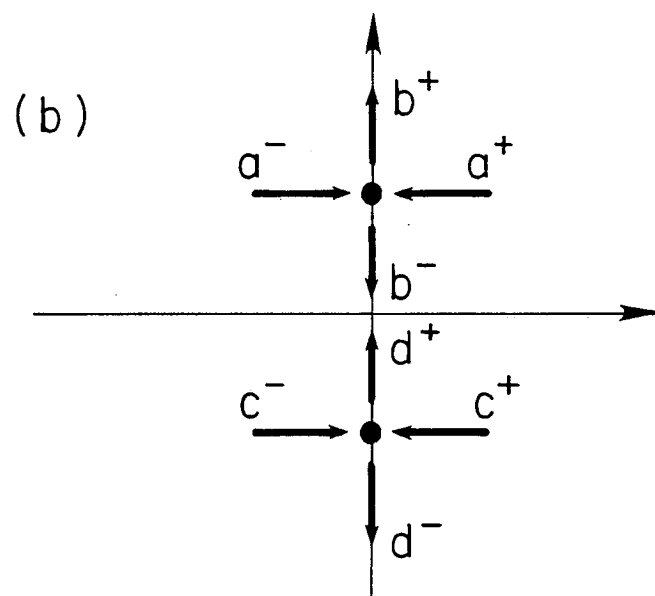
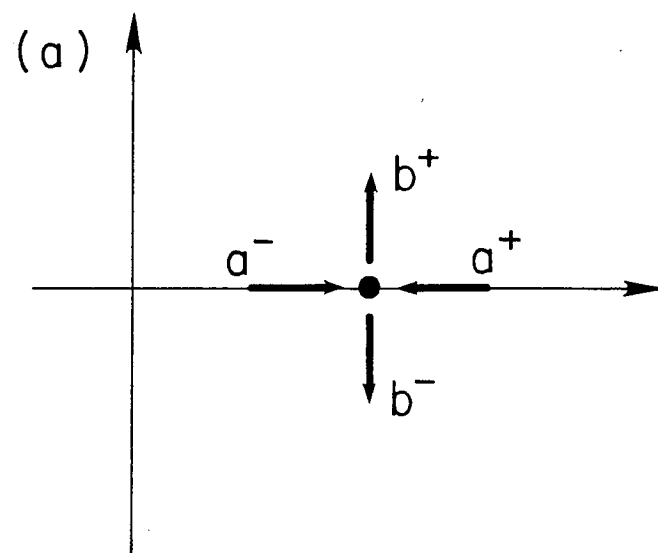


Fig. 3

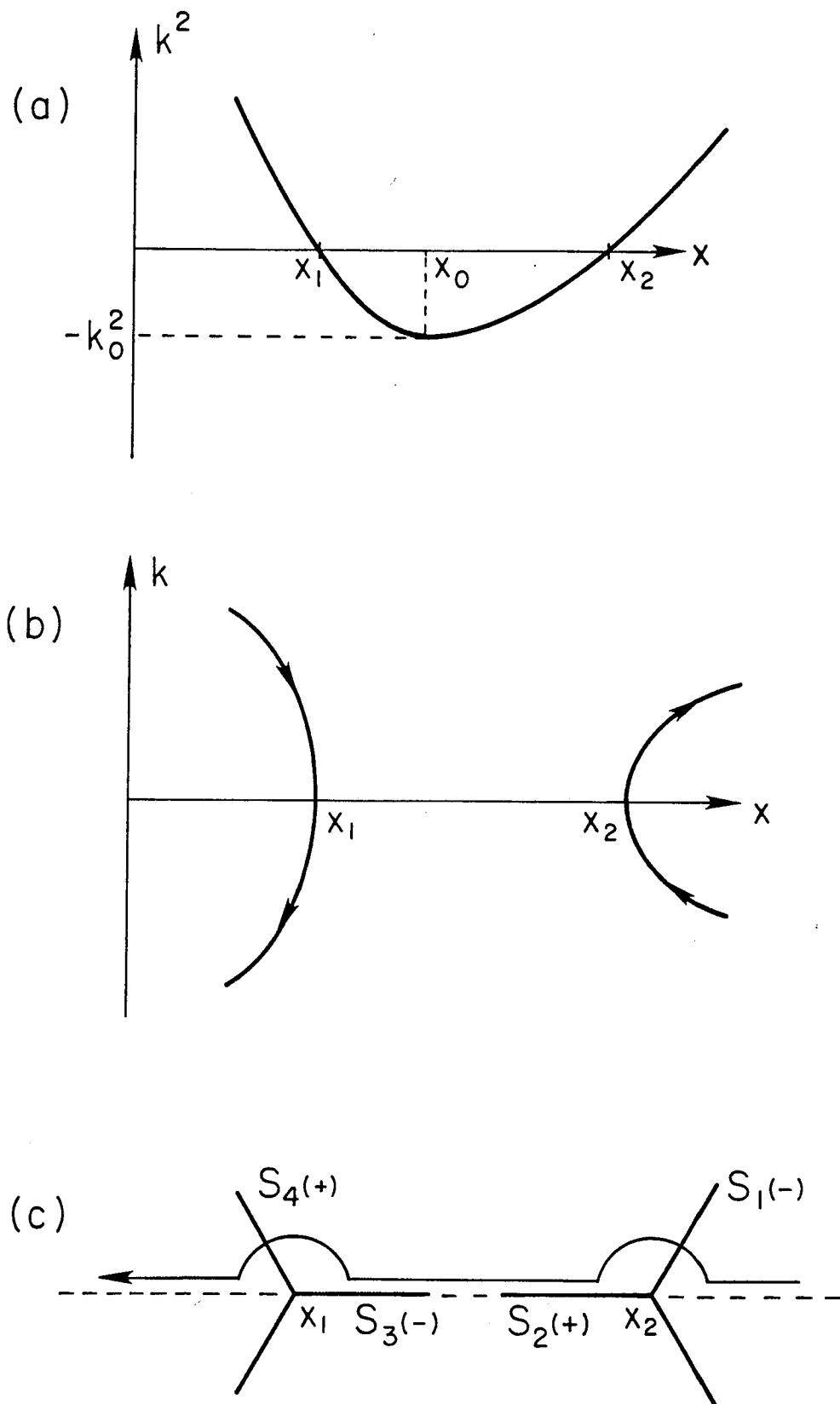


Fig. 4

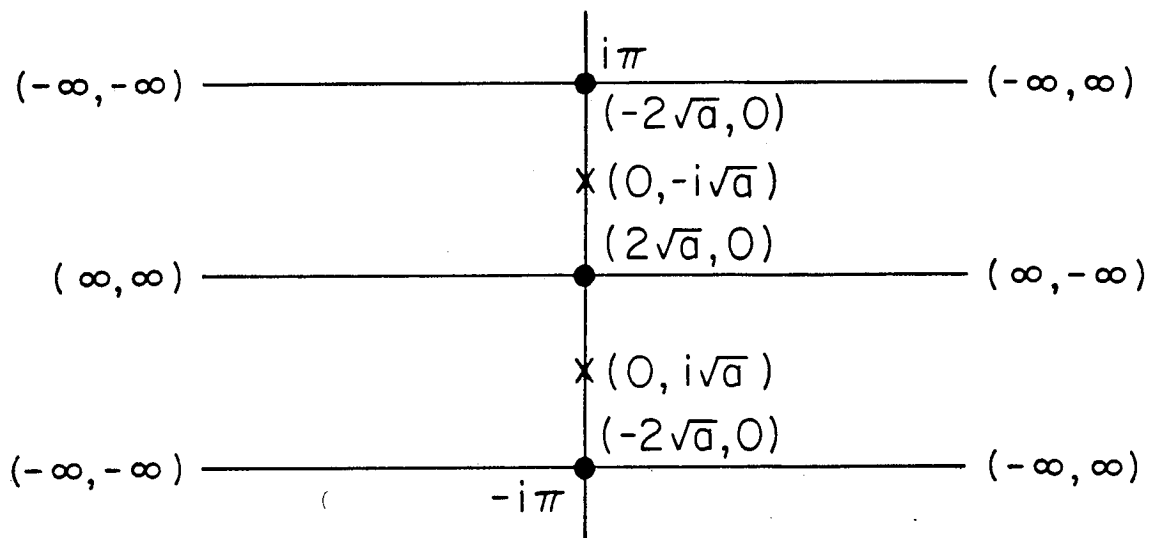


Fig. 5

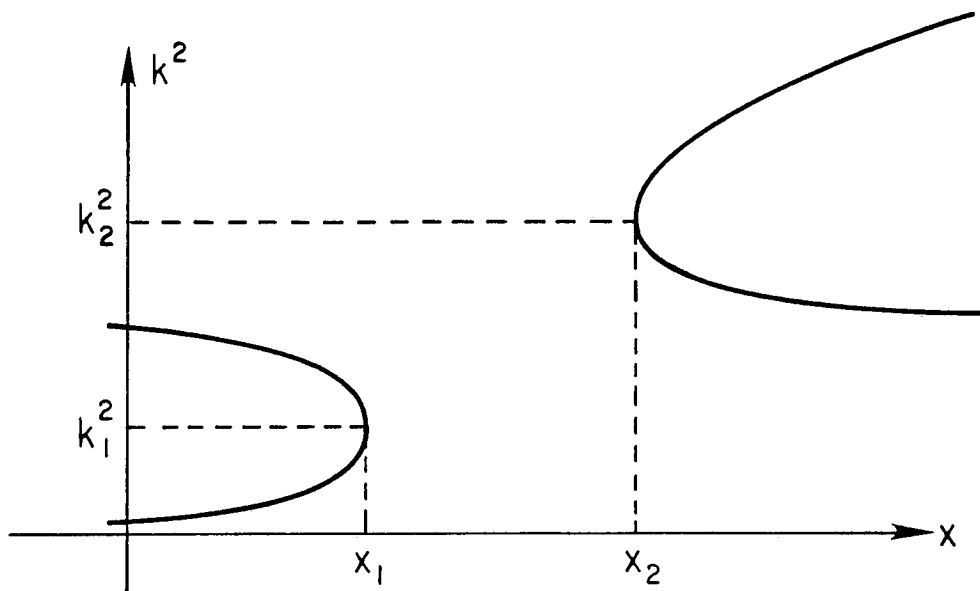


Fig. 6

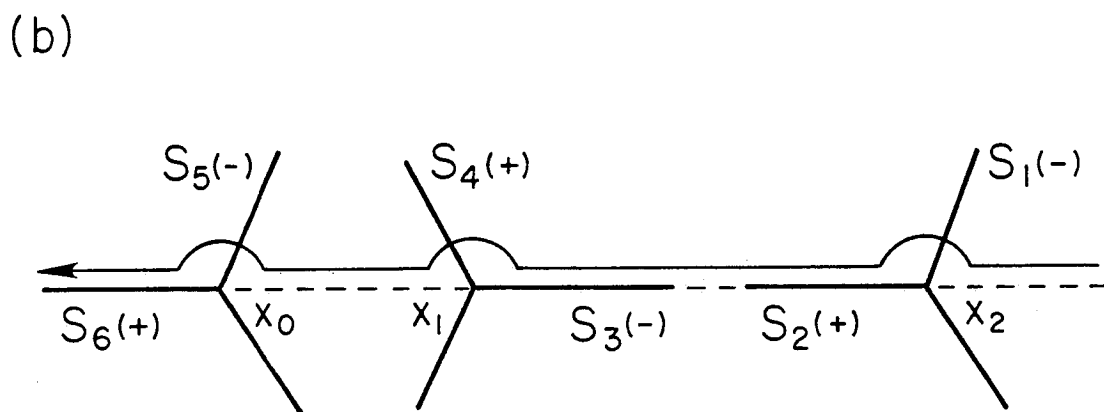
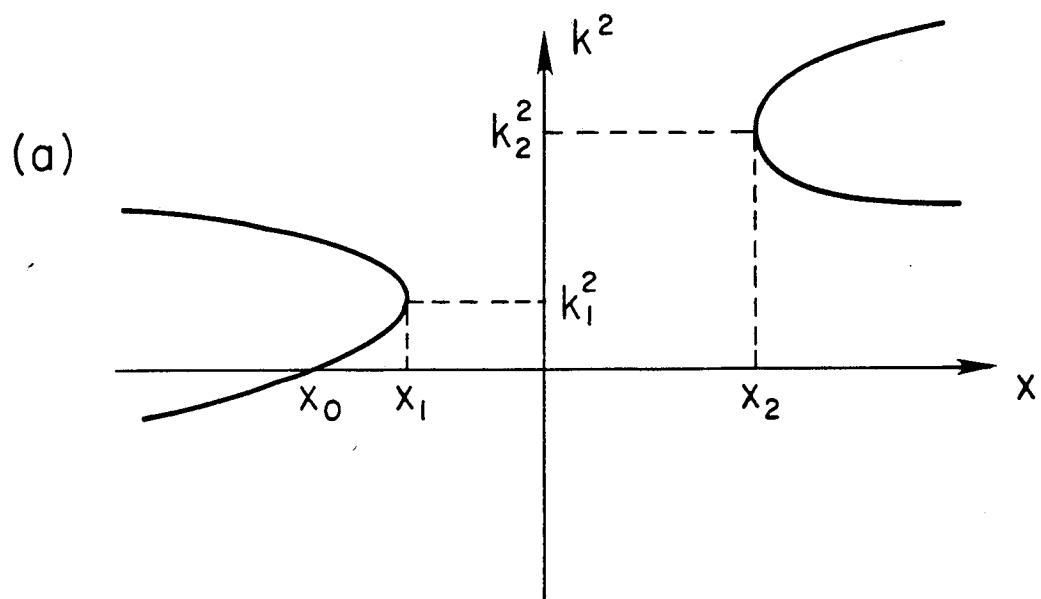
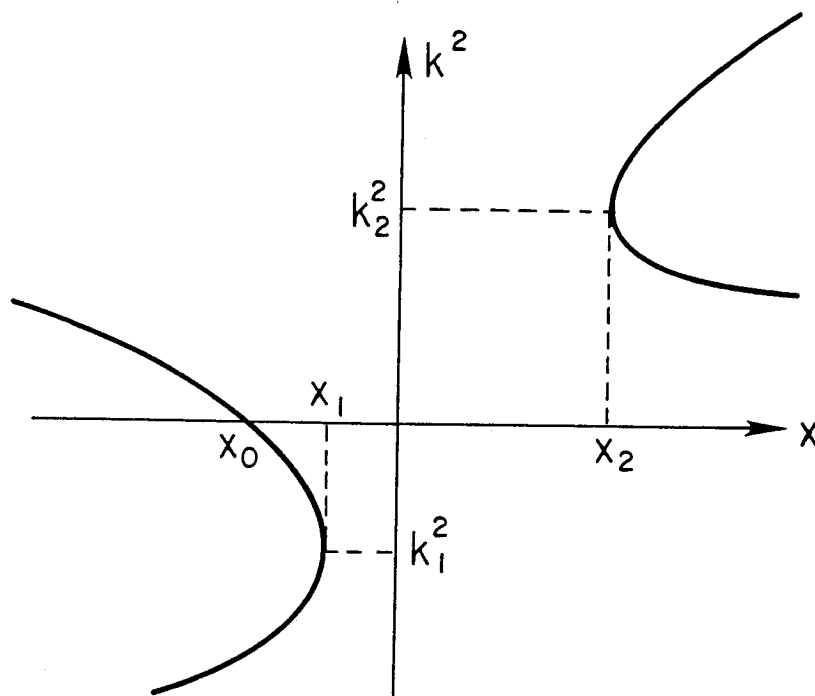


Fig. 7

(a)



(b)

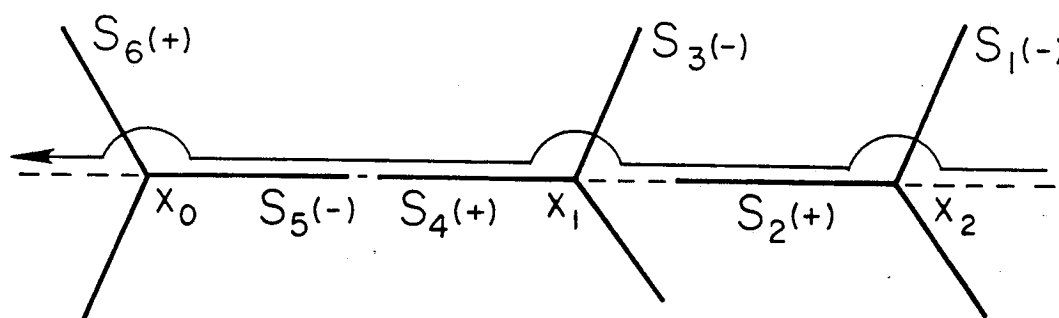


Fig. 8

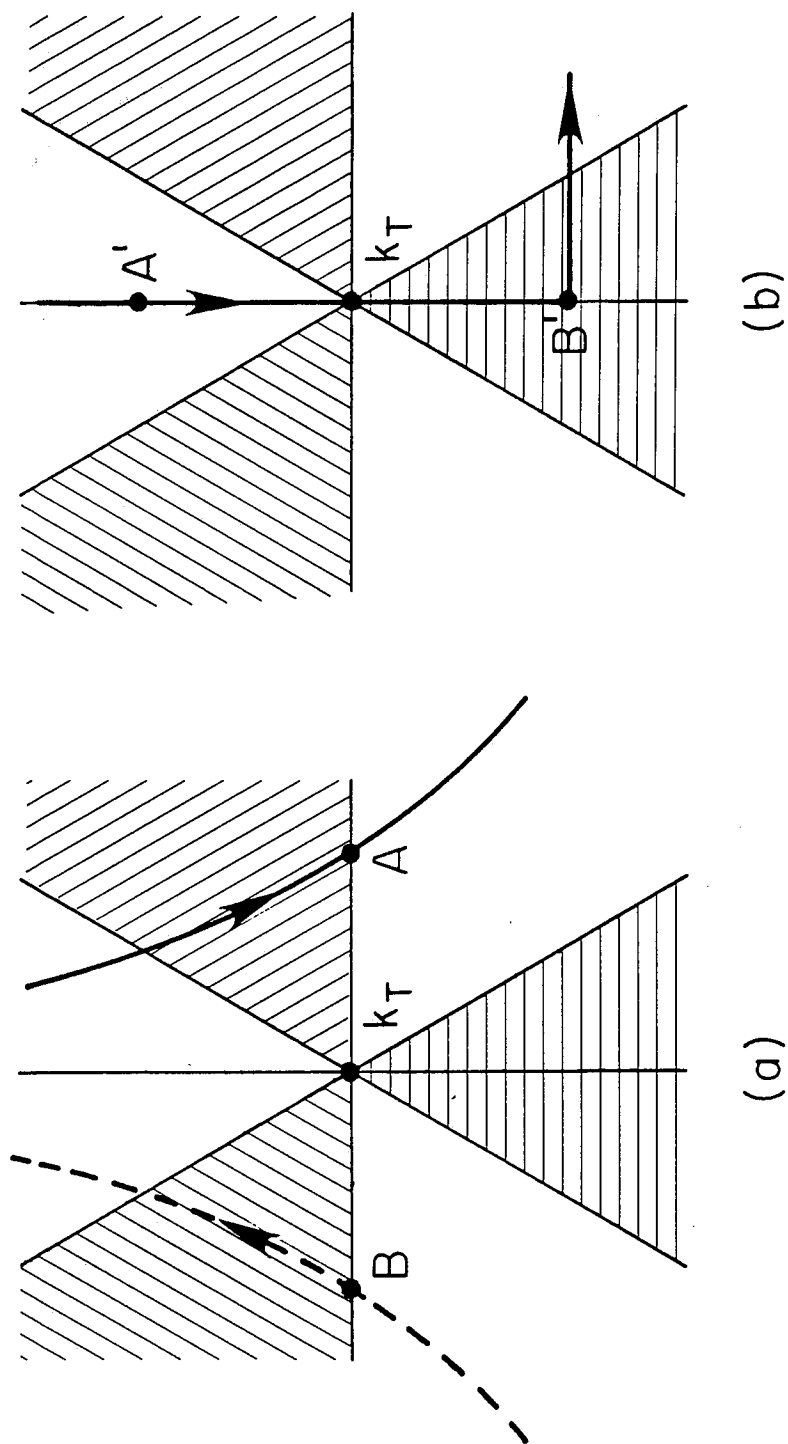
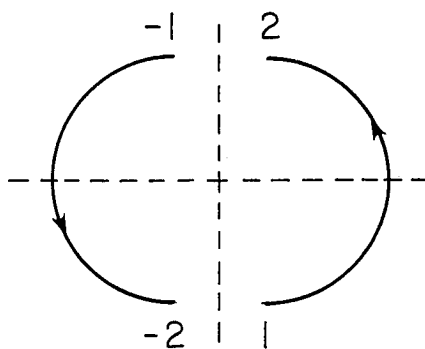


Fig. 9

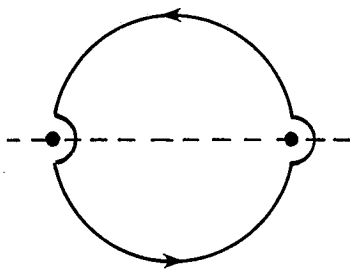
(18)

$$\text{circle with } \bullet = e^{-i\pi}, \quad \text{circle with } \times = 1$$

(19)

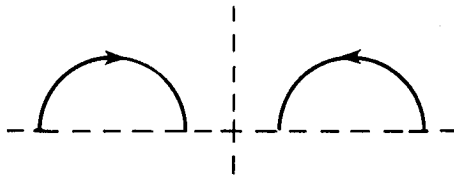


(20)



$$\left(\text{circle from } 2 \text{ to } 1 \text{ above axis} \right) \circ \left(\text{circle from } 1 \text{ to } 2 \text{ below axis} \right)^{-1}$$

page 27
(22 b)?

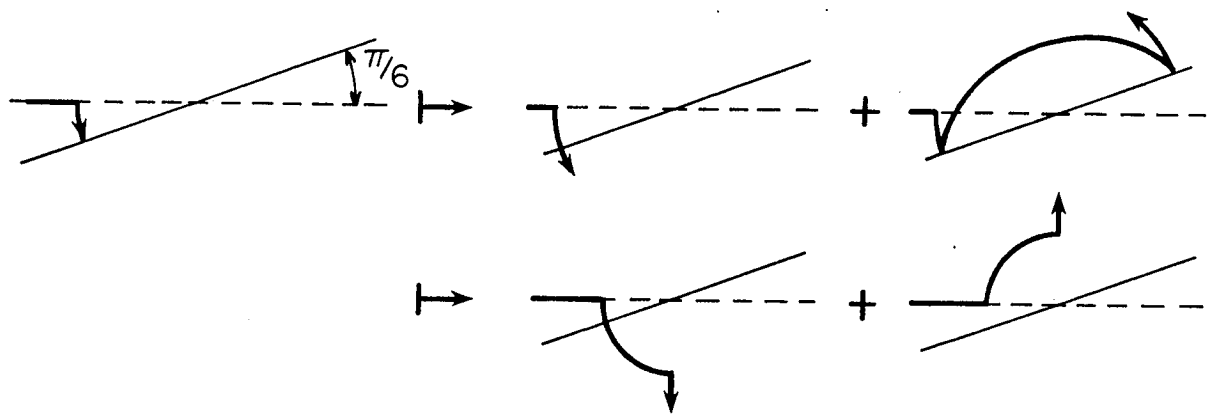


(23)

see insertion (next page)

(25)

(26)



(40)

$$\begin{aligned}
 2B^+(B^-)^* &= \text{diagram 1} |A^+|^2 + \text{diagram 2} |A^-|^2 \\
 &+ \text{diagram 3} A^+(A^-)^* + \text{diagram 4} A^-(A^+)^*
 \end{aligned}$$

The diagrams are as follows:

- Diagram 1: A horizontal dashed line with a vertical solid line in the center. On the left side, there is a dot on the line with a curved arrow pointing down and to the left. On the right side, there is a dot on the line with a curved arrow pointing up and to the right.
- Diagram 2: A horizontal dashed line with a vertical solid line in the center. On the left side, there is a dot on the line with a curved arrow pointing down and to the left. On the right side, there is a dot on the line with a curved arrow pointing up and to the right.
- Diagram 3: A horizontal dashed line with a vertical solid line in the center. On the left side, there is a dot on the line with a curved arrow pointing down and to the left. On the right side, there is a dot on the line with a curved arrow pointing up and to the right.
- Diagram 4: A horizontal dashed line with a vertical solid line in the center. On the left side, there is a dot on the line with a curved arrow pointing down and to the left. On the right side, there is a dot on the line with a curved arrow pointing up and to the right.

$$\text{diagram 1} = \frac{D_{,a^+}}{D_{,b^+}}, \quad \text{diagram 2} = \frac{D_{,a^-}}{D_{,b^+}},$$

(41)

$$\text{diagram 1} = -\frac{D_{,b^-}}{D_{,b^+}} \left(\text{diagram 2} \right)^*$$

(43)

$$2B^+D^{-*} = \begin{array}{c} \uparrow \\ \bullet \\ \text{---} \\ \downarrow \end{array} A^+C^{+*} + \begin{array}{c} \uparrow \\ \bullet \\ \text{---} \\ \downarrow \end{array} A^-C^{-*} +$$

$$+ \begin{array}{c} \uparrow \\ \bullet \\ \text{---} \\ \downarrow \end{array} A^+C^{-*} + \begin{array}{c} \uparrow \\ \bullet \\ \text{---} \\ \downarrow \end{array} A^-C^{+*}$$

$$2B^-D^{+*} = \begin{array}{c} \bullet \\ \downarrow \\ \text{---} \\ \uparrow \end{array} A^+C^{+*} + \begin{array}{c} \bullet \\ \downarrow \\ \text{---} \\ \uparrow \end{array} A^-C^{-*} +$$

$$+ \begin{array}{c} \bullet \\ \downarrow \\ \text{---} \\ \uparrow \end{array} A^+C^{-*} + \begin{array}{c} \bullet \\ \downarrow \\ \text{---} \\ \uparrow \end{array} A^-C^{+*}$$

(44)

$$\begin{array}{c} \bullet \\ \downarrow \\ \text{---} \\ \uparrow \end{array} = - \begin{array}{c} \bullet \\ \downarrow \\ \text{---} \\ \uparrow \end{array} ; \quad \begin{array}{c} \bullet \\ \downarrow \\ \text{---} \\ \uparrow \end{array} = - \begin{array}{c} \bullet \\ \downarrow \\ \text{---} \\ \uparrow \end{array}$$

(45)

$$\begin{array}{c} \uparrow \\ \bullet \\ \text{---} \\ \bullet \\ \downarrow \end{array} = \frac{D_{,a^+}}{D_{,b^+}}, \quad \begin{array}{c} \uparrow \\ \bullet \\ \text{---} \\ \bullet \\ \downarrow \end{array} = \frac{D_{,a^-}}{D_{,b^+}}$$

$$\begin{array}{c} \uparrow \\ \bullet \\ \text{---} \\ \bullet \\ \downarrow \end{array} = \frac{D_{,a^+}}{D_{,b^-}}, \quad \begin{array}{c} \uparrow \\ \bullet \\ \text{---} \\ \bullet \\ \downarrow \end{array} = \frac{D_{,a^-}}{D_{,b^-}}$$

(46)

$$\bullet \leftarrow \xrightarrow{S_2} \begin{array}{c} \uparrow \\ \bullet \\ \text{---} \\ \bullet \\ \downarrow \end{array} + \frac{1}{2} \begin{array}{c} \uparrow \\ \bullet \\ \text{---} \\ \bullet \\ \downarrow \end{array}$$

$$\xrightarrow{S_3} \frac{1}{2} \begin{array}{c} \uparrow \\ \bullet \\ \text{---} \\ \bullet \\ \downarrow \end{array} + (1 - \frac{1}{4}q) \begin{array}{c} \textcircled{x} \\ | \\ \bullet \\ \text{---} \\ \bullet \\ \downarrow \end{array}$$

$$\xrightarrow{S_4} (1 + \frac{1}{4}q) \begin{array}{c} \textcircled{x} \\ | \\ \bullet \\ \text{---} \\ \bullet \\ \downarrow \end{array} + (1 - \frac{1}{4}q) \begin{array}{c} \textcircled{x} \\ | \\ \bullet \\ \text{---} \\ \bullet \\ \downarrow \end{array}$$

$$q = \begin{array}{c} \textcircled{x} \\ | \\ \bullet \\ \text{---} \\ \bullet \\ \text{---} \\ \bullet \\ | \\ \textcircled{x} \end{array} = e^{i\phi_{kdz}}$$

(50)

$$1 + \frac{1 - \frac{q}{4}}{1 + \frac{q}{4}} \rightarrow \text{diagram} \rightarrow \frac{\text{diagram}}{1 + \frac{q}{4}}$$

The diagram on the left is a horizontal line with a dot in the middle and a semi-circular arc above it pointing to the left. The diagram on the right is a horizontal line with a dot in the middle, a semi-circular arc above it pointing to the right, and a vertical line segment extending upwards from the dot to a circle containing an 'x'.

$$|\text{diagram}|^2 = \text{diagram} \text{diagram} = -\frac{D, k_i}{D, k_r}$$

The diagram in the first term is the same as in (50). The diagram in the second term consists of two circles, each containing an 'x', connected by a vertical line segment. The top circle is connected to a horizontal line with a dot and a semi-circular arc pointing left. The bottom circle is connected to a horizontal line with a dot and a semi-circular arc pointing right.

(51)

$$|\text{diagram}|^2 = \text{diagram} \text{diagram} = q \frac{D, k_i}{D, k_t}$$

The diagram in the first term is the same as in (50). The diagram in the second term consists of two circles, each containing an 'x', connected by a vertical line segment. The top circle is connected to a horizontal line with a dot and a semi-circular arc pointing left. The bottom circle is connected to a horizontal line with a dot and a semi-circular arc pointing right.

$$\frac{1}{2} \text{diagram} = -i e^{2iS_1}$$

The diagram is the same as in (50).

(58)

$$\text{diagram} = \sqrt{\frac{k_1}{k_2}} e^{-\pi a} e^{i(S_1 + S_2)}$$

The diagram is the same as in (50).

(68)

$$\begin{array}{c} \text{---} \curvearrowright \text{---} \\ \bullet \rightarrow \quad \bullet \end{array} \left(1 + \frac{1}{4}q\right) + \begin{array}{c} \text{---} \curvearrowleft \text{---} \\ \bullet \leftarrow \quad \bullet \end{array} \left(1 - \frac{1}{4}q\right)$$

$$q = \begin{array}{c} \curvearrowright \\ \bullet \quad \bullet \\ \curvearrowleft \end{array} = \sigma e^{i\oint k dz}$$

(69)

$$\left(1 + \frac{q}{4}\right) \begin{array}{c} \text{---} \curvearrowright \text{---} \\ \bullet \rightarrow \quad \bullet \end{array} + \left(1 - \frac{q}{4}\right) \left(\begin{array}{c} \text{---} \curvearrowright \text{---} \\ \bullet \leftarrow \quad \bullet \end{array} + \frac{1}{2} \begin{array}{c} \text{---} \curvearrowright \text{---} \\ \bullet \quad \bullet \end{array} \right)$$

(70)

$$\left(1 - \frac{q}{4}\right) \begin{array}{c} \text{---} \curvearrowleft \text{---} \\ \bullet \leftarrow \quad \bullet \end{array} + \left(1 + \frac{q}{4}\right) \left(\begin{array}{c} \text{---} \curvearrowleft \text{---} \\ \bullet \quad \bullet \end{array} + \frac{1}{2} \begin{array}{c} \text{---} \curvearrowleft \text{---} \\ \bullet \quad \bullet \end{array} \right)$$

(71)

$$\begin{array}{c} \curvearrowright \\ \bullet \quad \bullet \\ \curvearrowleft \end{array} - \begin{array}{c} \curvearrowright \\ \bullet \quad \bullet \\ \curvearrowleft \end{array} = \begin{array}{c} \curvearrowright \\ \bullet \quad \bullet \\ \curvearrowleft \end{array} - \begin{array}{c} \curvearrowright \\ \bullet \quad \bullet \\ \curvearrowleft \end{array} \circ \begin{array}{c} \curvearrowright \\ \bullet \quad \bullet \\ \curvearrowleft \end{array} = q$$

(72)

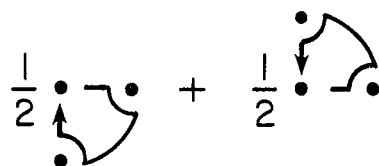
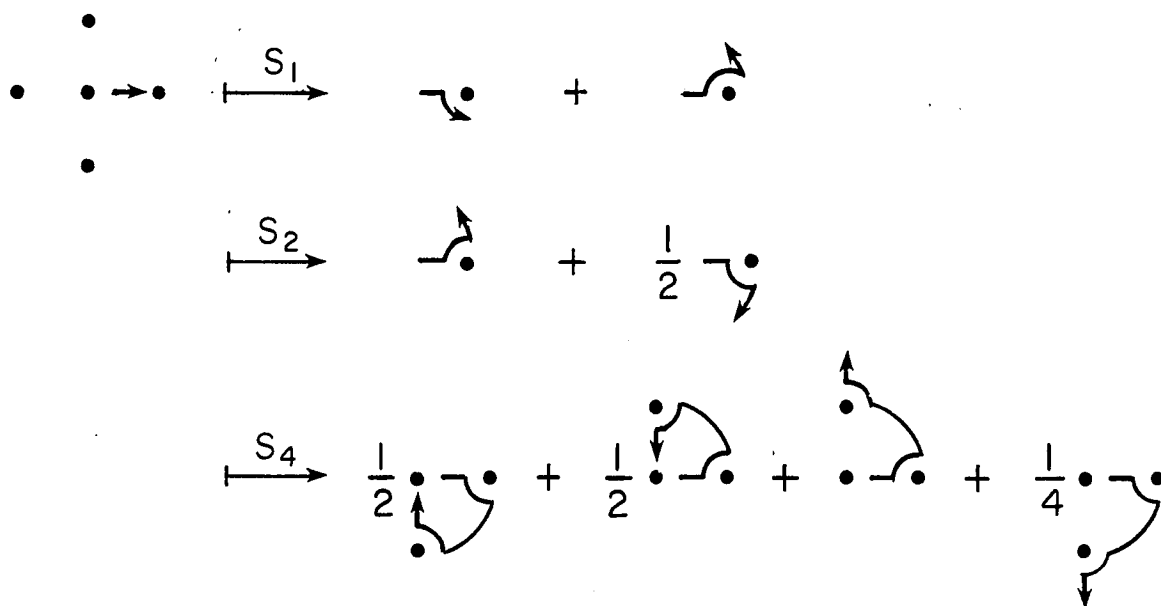
$r ; r = \frac{1 - \frac{q}{4}}{1 + \frac{q}{4}}$

$$1 + \text{diagram 1} \cdot r^2 + \text{diagram 2} \cdot r$$

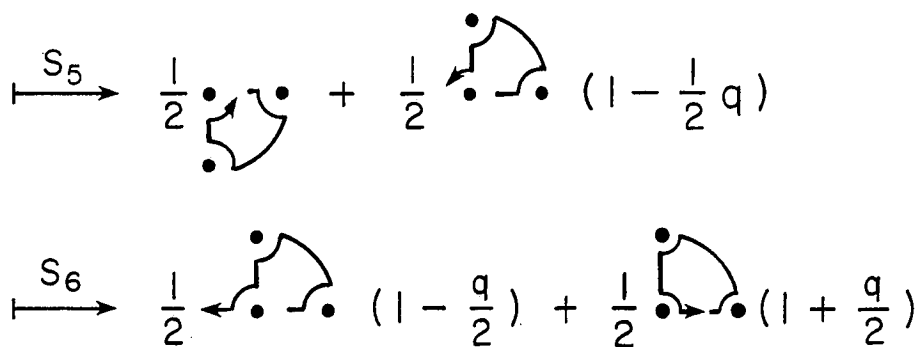
(73)

$$\rightarrow \frac{\text{Diagram 1}}{1 + \frac{q}{4}} + r \left[\text{Diagram 2} \right] \frac{\text{Diagram 3}}{1 + \frac{q}{4}}$$


(75)



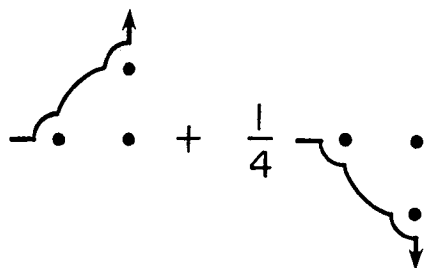
(76)



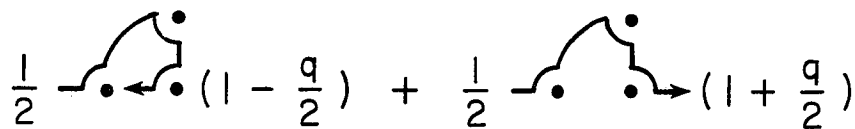
(77)

$$q = \oint = \sigma e^{i\oint k dz}$$


(78)

$$- \frac{1}{4} + \frac{1}{4}$$


(79)

$$\frac{1}{2} \left(1 - \frac{q}{2} \right) + \frac{1}{2} \left(1 + \frac{q}{2} \right)$$


(80)



(21)

$$\begin{array}{c} \bullet \\ \uparrow \\ \bullet \end{array} \begin{array}{c} \bullet \\ \text{---} \\ \bullet \end{array} \left(1 + \begin{array}{c} \bullet \\ \text{---} \leftarrow \bullet \end{array} \begin{array}{c} \bullet \\ \text{---} \\ \bullet \end{array} \begin{array}{c} \bullet \\ \text{---} \leftarrow \bullet \end{array} \begin{array}{c} \bullet \\ \text{---} \\ \bullet \end{array} \right) = 0$$

$$\begin{array}{c} \bullet \\ \text{---} \\ \bullet \end{array} \begin{array}{c} \bullet \\ \text{---} \\ \bullet \end{array} \left(1 + \begin{array}{c} \bullet \\ \text{---} \leftarrow \bullet \end{array} \begin{array}{c} \bullet \\ \text{---} \\ \bullet \end{array} \begin{array}{c} \bullet \\ \text{---} \leftarrow \bullet \end{array} \begin{array}{c} \bullet \\ \text{---} \\ \bullet \end{array} \right) = 0$$

(22)

$$1 + \frac{1 - \frac{q}{2}}{1 + \frac{q}{2}} \begin{array}{c} \bullet \\ \text{---} \leftarrow \bullet \end{array} \begin{array}{c} \bullet \\ \text{---} \\ \bullet \end{array} \begin{array}{c} \bullet \\ \text{---} \\ \bullet \end{array} \begin{array}{c} \bullet \\ \text{---} \\ \bullet \end{array} \longrightarrow \frac{\begin{array}{c} \bullet \\ \text{---} \leftarrow \bullet \end{array} \begin{array}{c} \bullet \\ \text{---} \\ \bullet \end{array}}{1 + \frac{q}{2}} + \frac{\begin{array}{c} \bullet \\ \text{---} \leftarrow \bullet \end{array} \begin{array}{c} \bullet \\ \text{---} \\ \bullet \end{array}}{1 + \frac{q}{2}}$$

$$A^{-}(\rightarrow \bullet) + A^{+}(\bullet \leftarrow) \xrightarrow{S_1} A^{-}(\searrow \bullet + \swarrow \bullet) + A^{+}(\bullet \nearrow)$$

$$\xrightarrow{S_2} A^{+}(\bullet \nwarrow + \frac{1}{2} \bullet \swarrow) + A^{-}(\swarrow \bullet + \nwarrow \bullet + \frac{1}{2} \bullet \searrow)$$

$$= A^{+}(\bullet \nwarrow + \frac{1}{2} \bullet \swarrow) + A^{-}(\swarrow \bullet + \frac{1}{2} \nwarrow \bullet)$$

